

Deciphering the desiccation trend of the South Asian monsoon hydroclimate in a warming world

R. Krishnan

Centre for Climate Change Research (CCCR)
Indian Institute of Tropical Meteorology, Pune

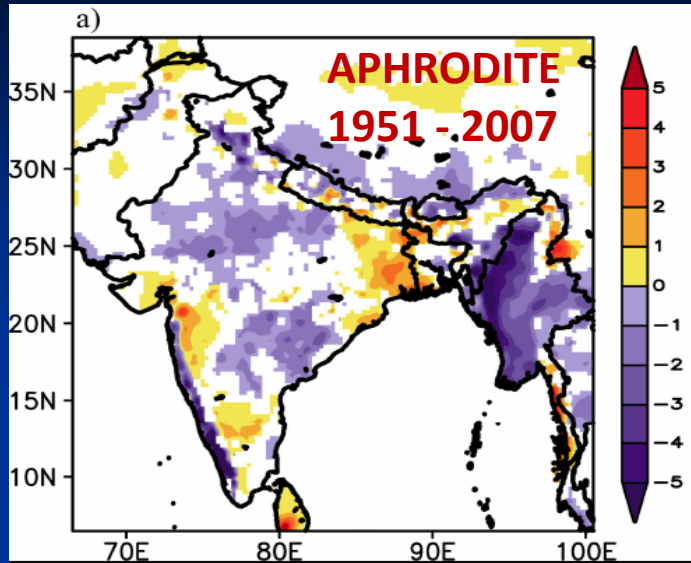
Collaborators: T.P. Sabin, R. Vellore, M. Mujumdar, J. Sanjay, B.N.Goswami

J.-L. Dufresne, F. Hourdin, P. Terray

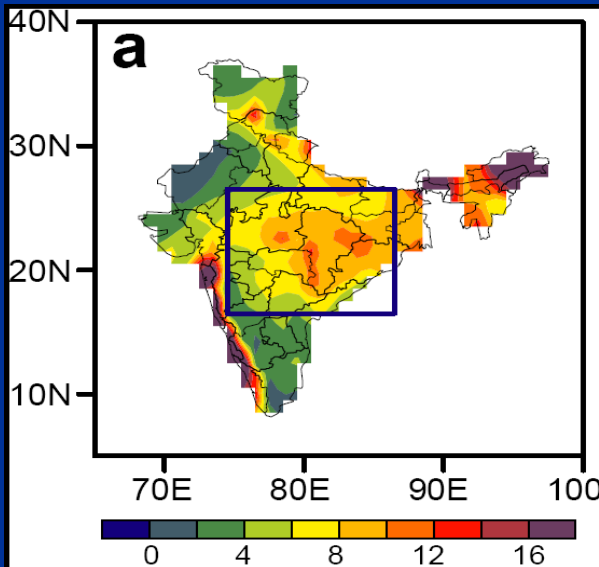
Annual Monsoon Workshop & National Symposium on Understanding and Forecasting of Monsoon Extremes

Indian Meteorological Society Pune Chapter, IITM, Pune 23-24 February, 2016

Spatial map of linear trend JJAS rainfall (1951 – 2007)

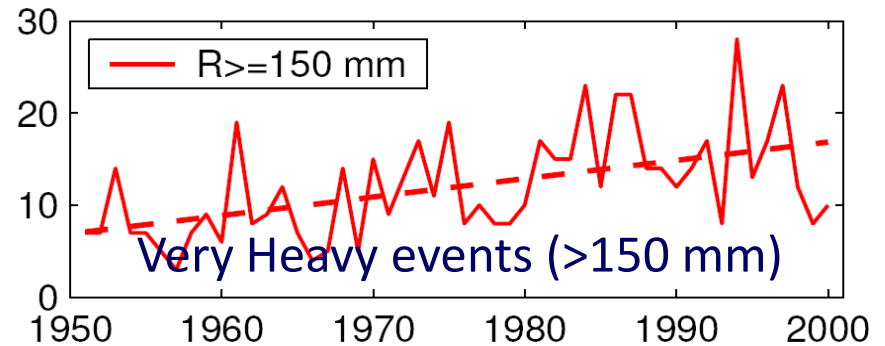
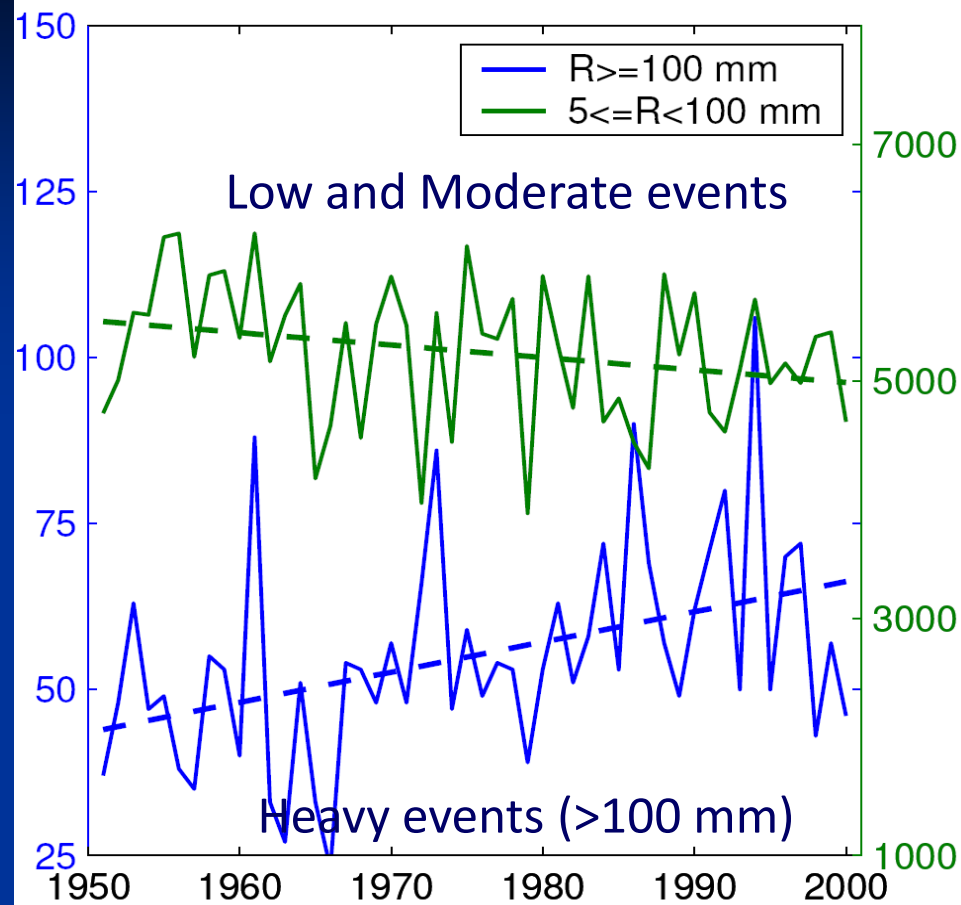


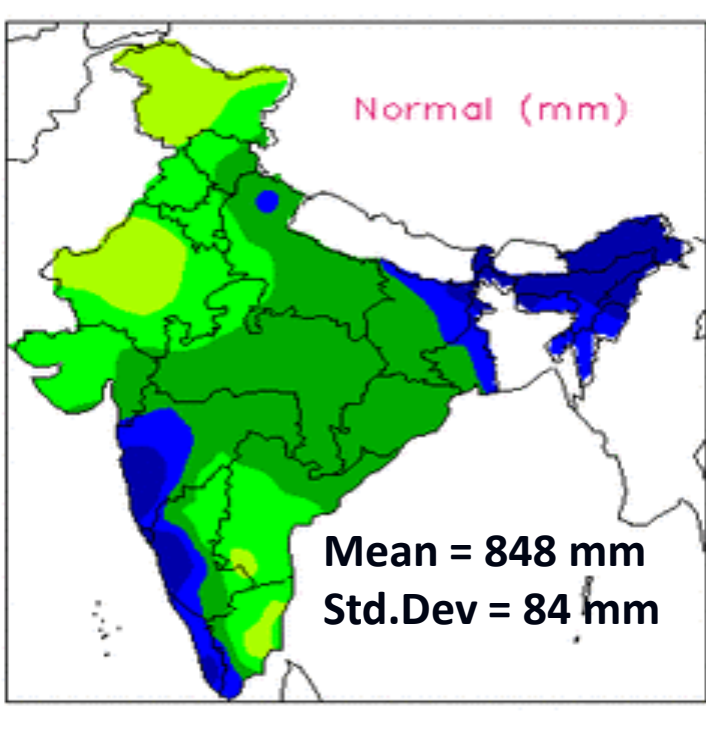
Increasing Trend of Extreme Rain Events over India in a Warming Environment



Goswami et al.
2006, Science

Time series of count over Central India



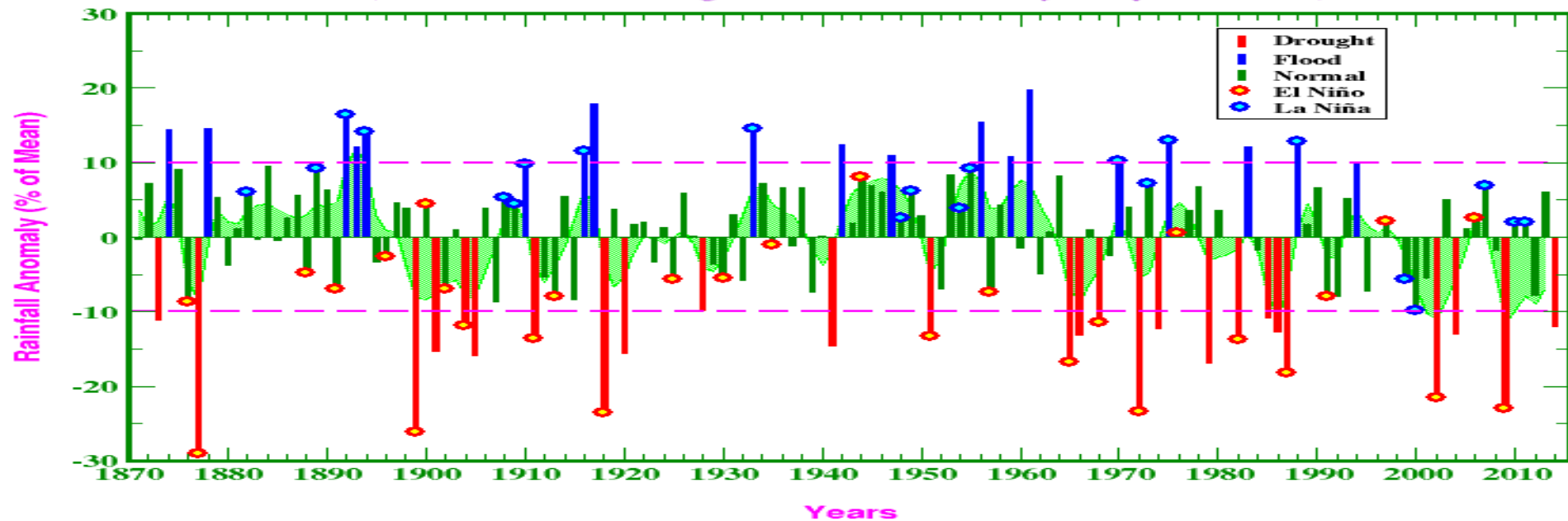


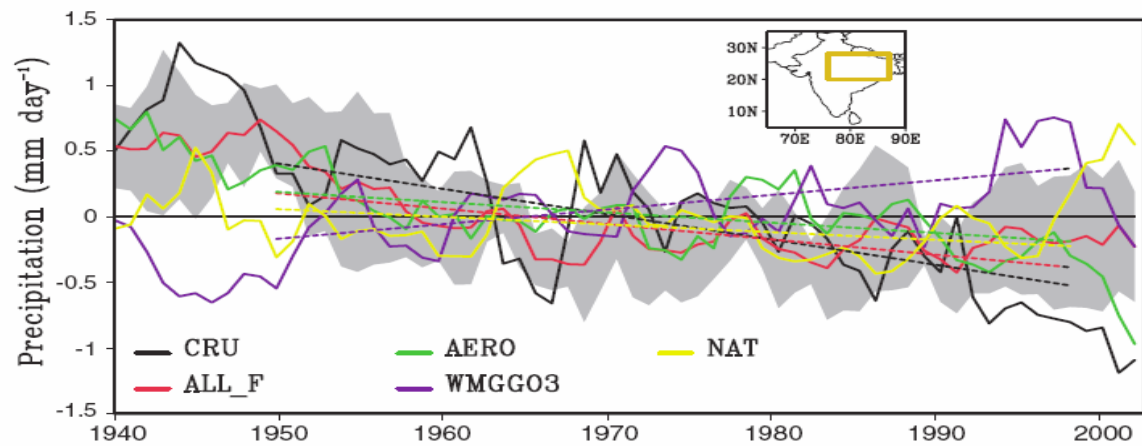
Long-term climatology of total rainfall over India during (1 Jun - 30 Sep) summer monsoon season (<http://www.tropmet.res.in>)

Interannual variability of the Indian Summer Monsoon Rainfall

All-India Summer Monsoon Rainfall, 1871-2014

(Based on IITM Homogeneous Indian Monthly Rainfall Data Set)





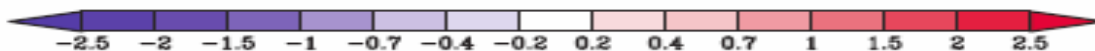
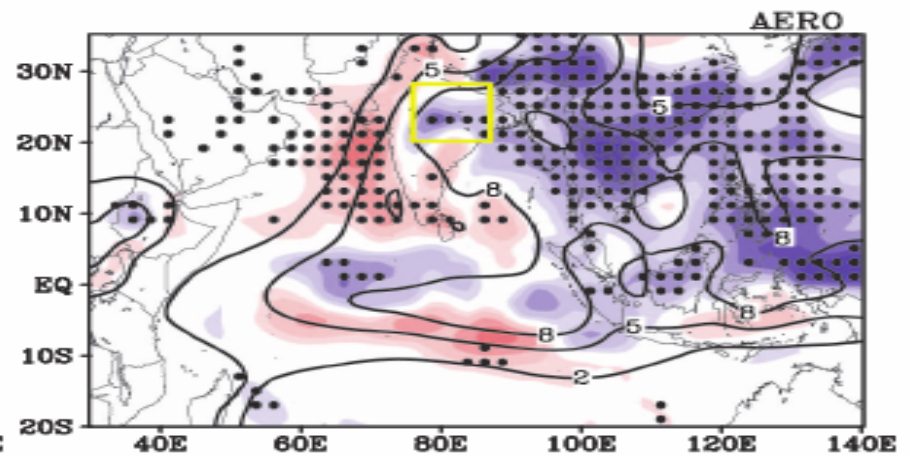
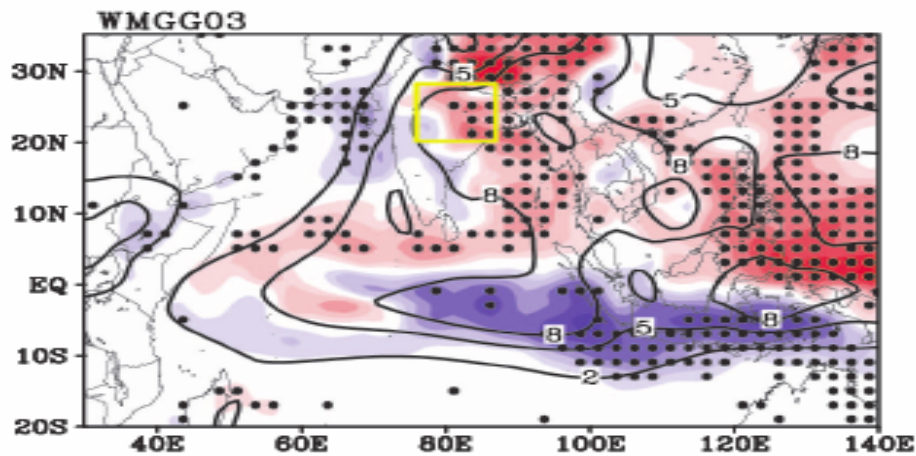
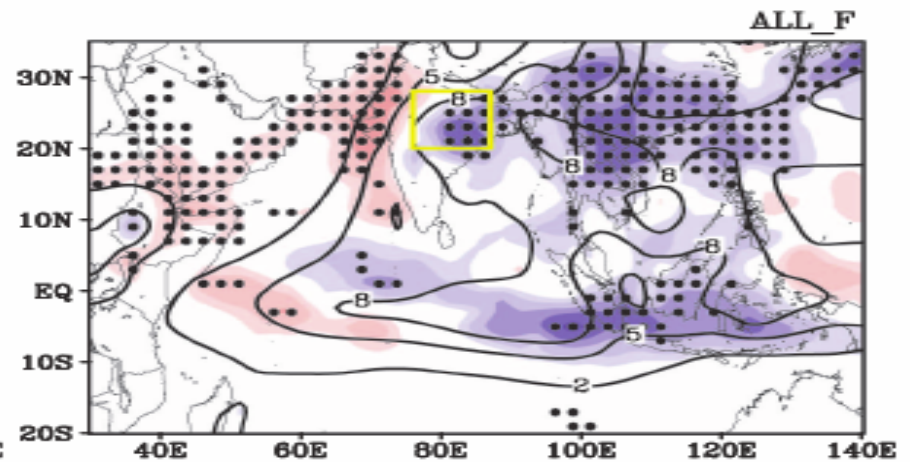
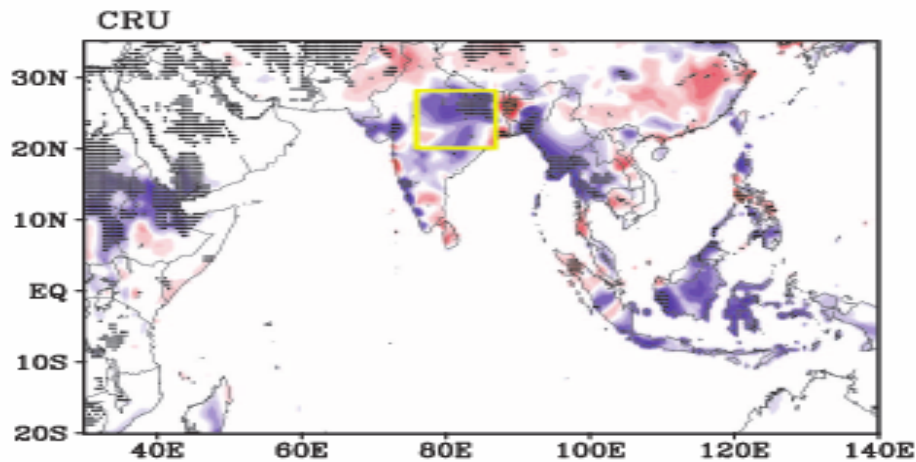
Anthropogenic Aerosols and the Weakening of the South Asian Summer Monsoon

Massimo A. Bollasina et al.

Science **334**, 502 (2011);

DOI: 10.1126/science.1204994

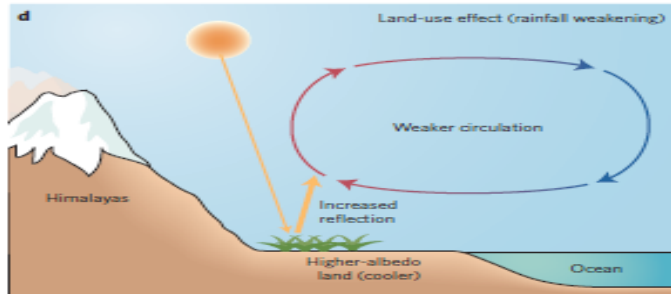
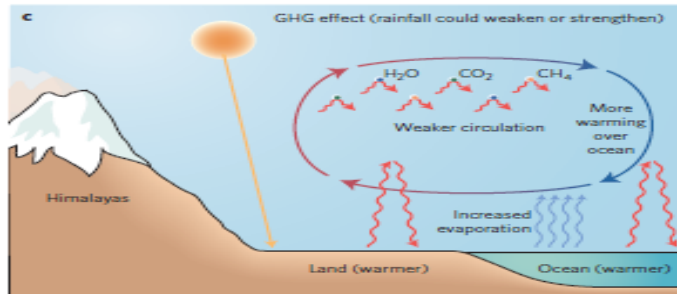
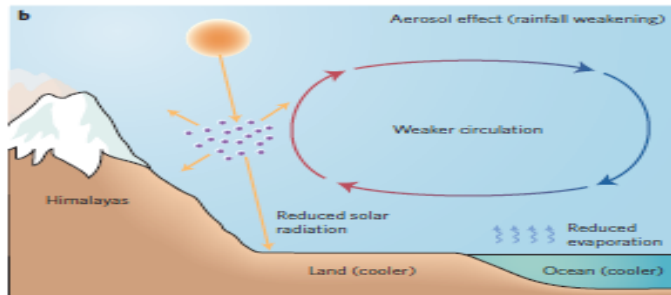
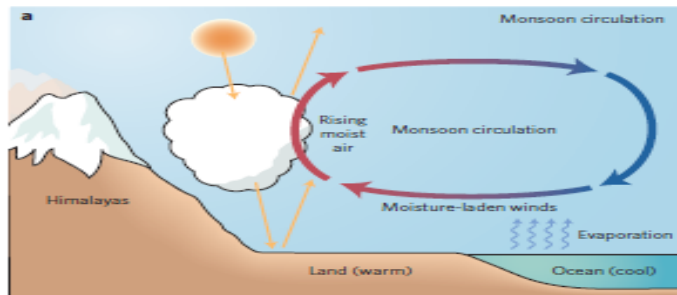
**Bollasina, Ming and Ramaswamy
Science, 2011**



Deciphering the desiccation trend of the South Asian monsoon hydroclimate in a warming world

R. Krishnan¹ · T. P. Sabin¹ · R. Vellore¹ · M. Mujumdar¹ · J. Sanjay¹ ·
B. N. Goswami^{1,2} · F. Hourdin³ · J.-L. Dufresne³ · P. Terray^{4,5}

news & views



The onset of the monsoon in early June brings with it a burst of life across the region — children playing on the streets, blossoming flora, flowing rivers, and sowing of agricultural lands. The monsoon supplies ~80% of South Asia's annual rainfall, supporting the region's primarily rain-fed agriculture and recharging rivers, aquifers and reservoirs that provide water to over one-fifth of the global population. Since the 1950s, the monsoon has weakened and become more erratic, with increased occurrence of extreme rainfall events². This has led to crop failures and water shortages with severe socio-economic and humanitarian impacts across South Asia. Writing in *Climate Dynamics*, R. Krishnan and colleagues³ suggest that anthropogenic greenhouse gas (GHG) emissions, aerosol emissions and agricultural land-cover changes are responsible for the observed changes in rainfall patterns. They predict that the monsoon weakening will continue through the twenty-first century, threatening the livelihoods and resources of over 1.6 billion people in the region.

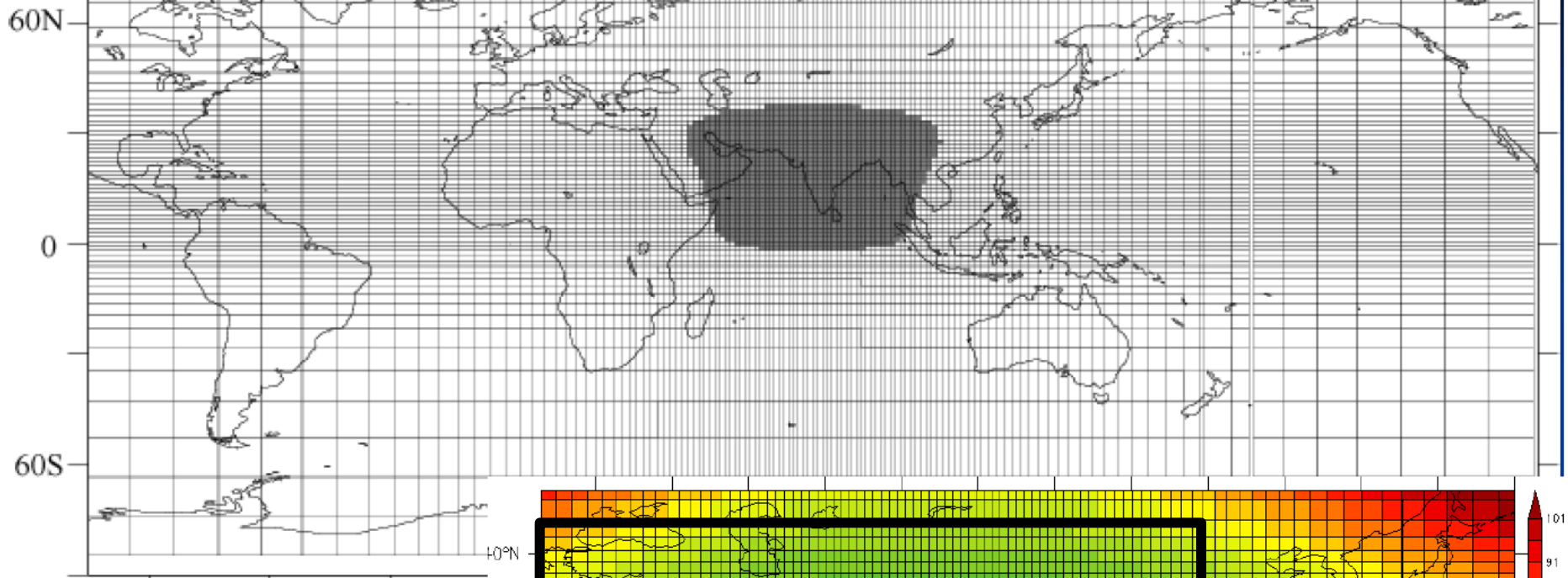
news & views

SOUTH ASIAN MONSOON

Tug of war on rainfall changes

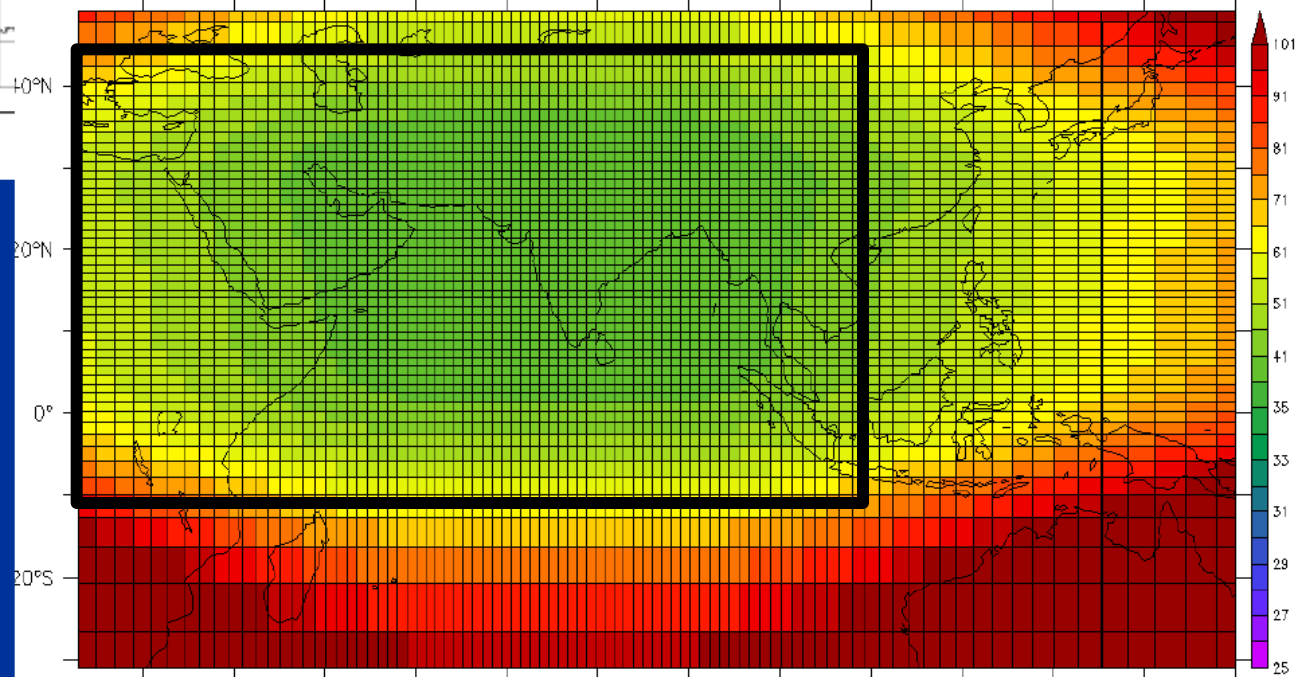
Rainfall associated with the South Asian summer monsoon has decreased by approximately 7% since 1950, but the reasons for this are unclear. Now research suggests that changes in land-cover patterns and increased emissions from human activities have contributed to this weakening, which is expected to continue in the coming decades.

LMDZ grid setup for CORDEX South Asia (shaded region has grid-size < 35 km)



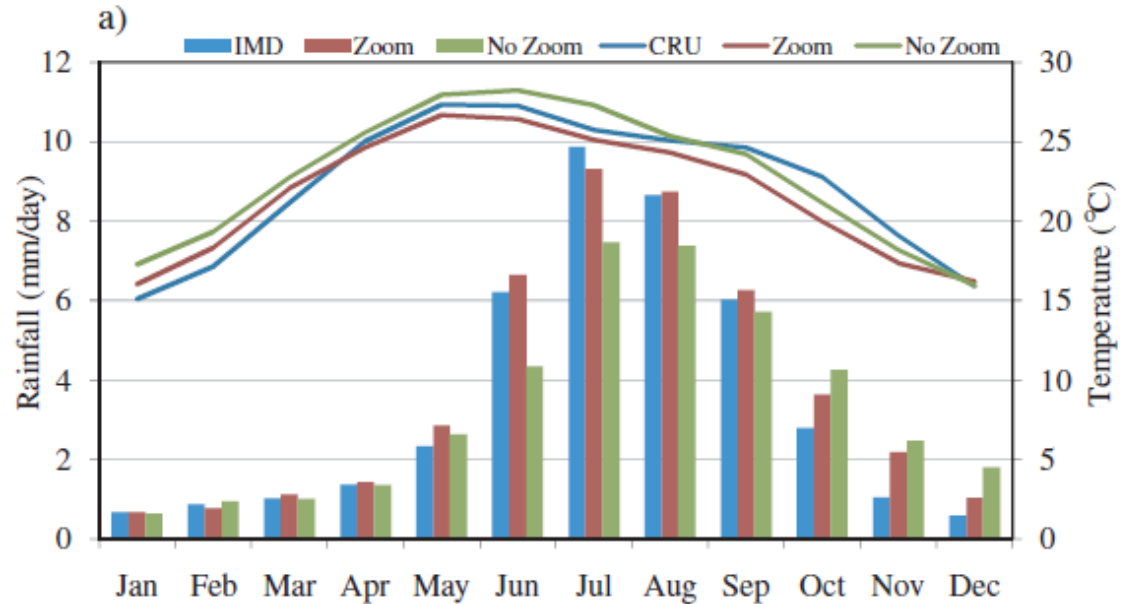
LMDZ global atmospheric model: Variable resolution with zooming capability

Source: Sabin, CCCR, IITM

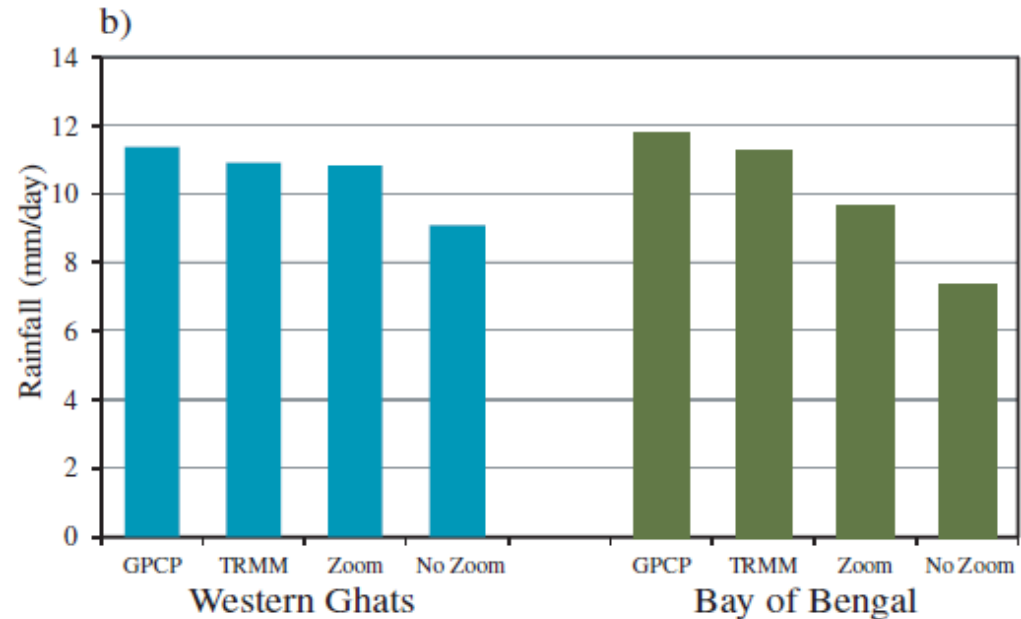


Climatological results

Rainfall and surface temperature over the Indian landmass



JJAS mean rainfall



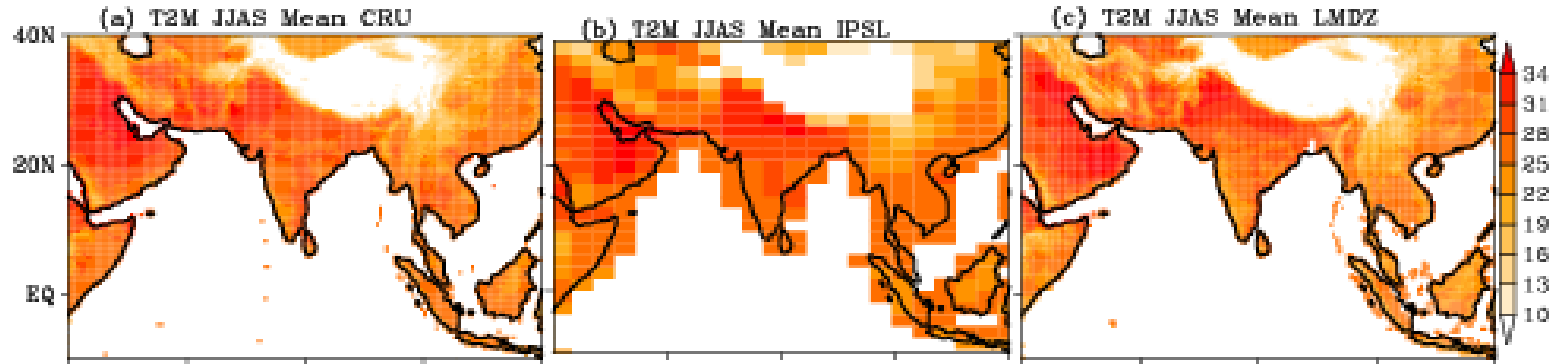
JJAS mean (1951-2005): Source: Ramarao et al. (2015) Earth Sys. Dynam

OBS

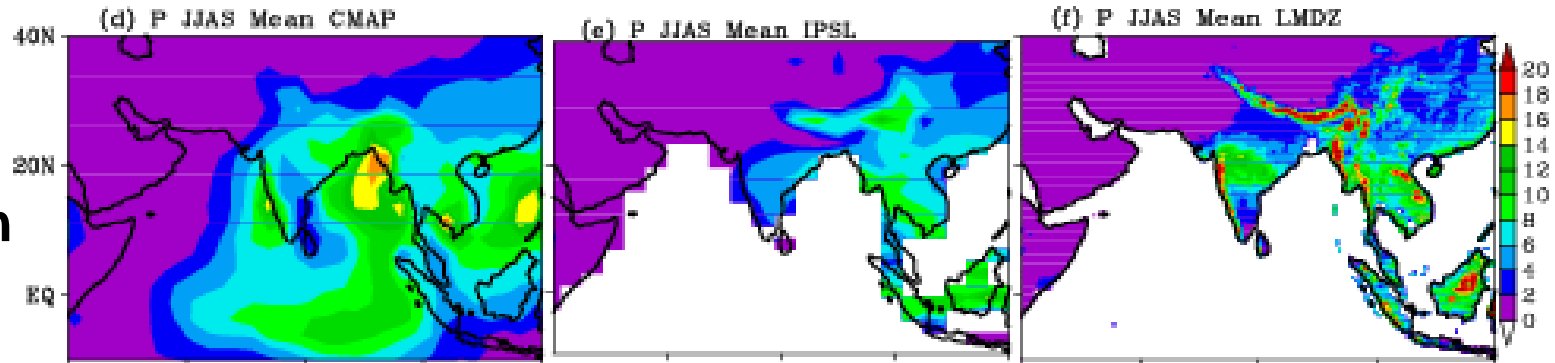
IPSL

LMDZ4

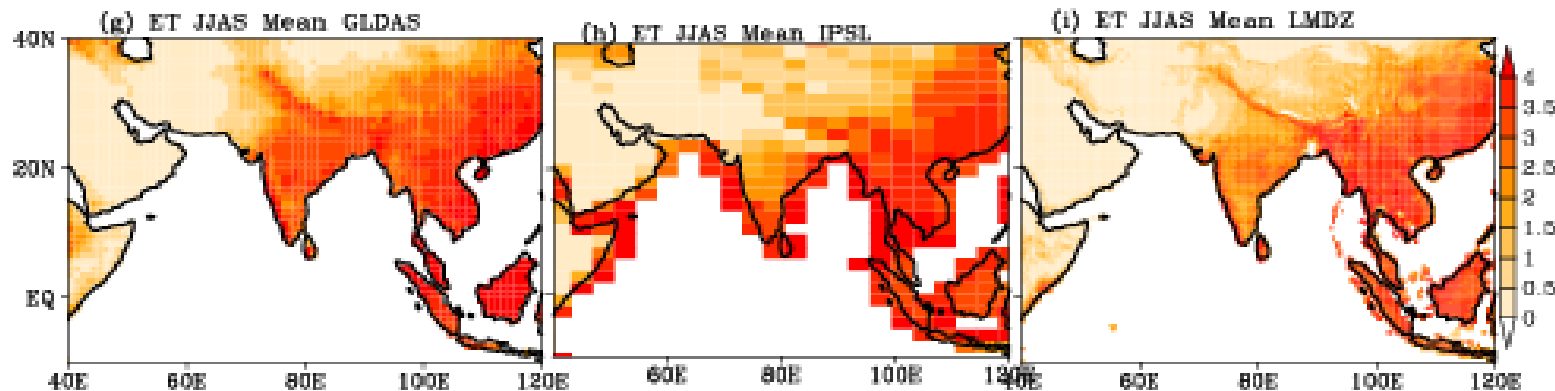
T2M



Precipitation



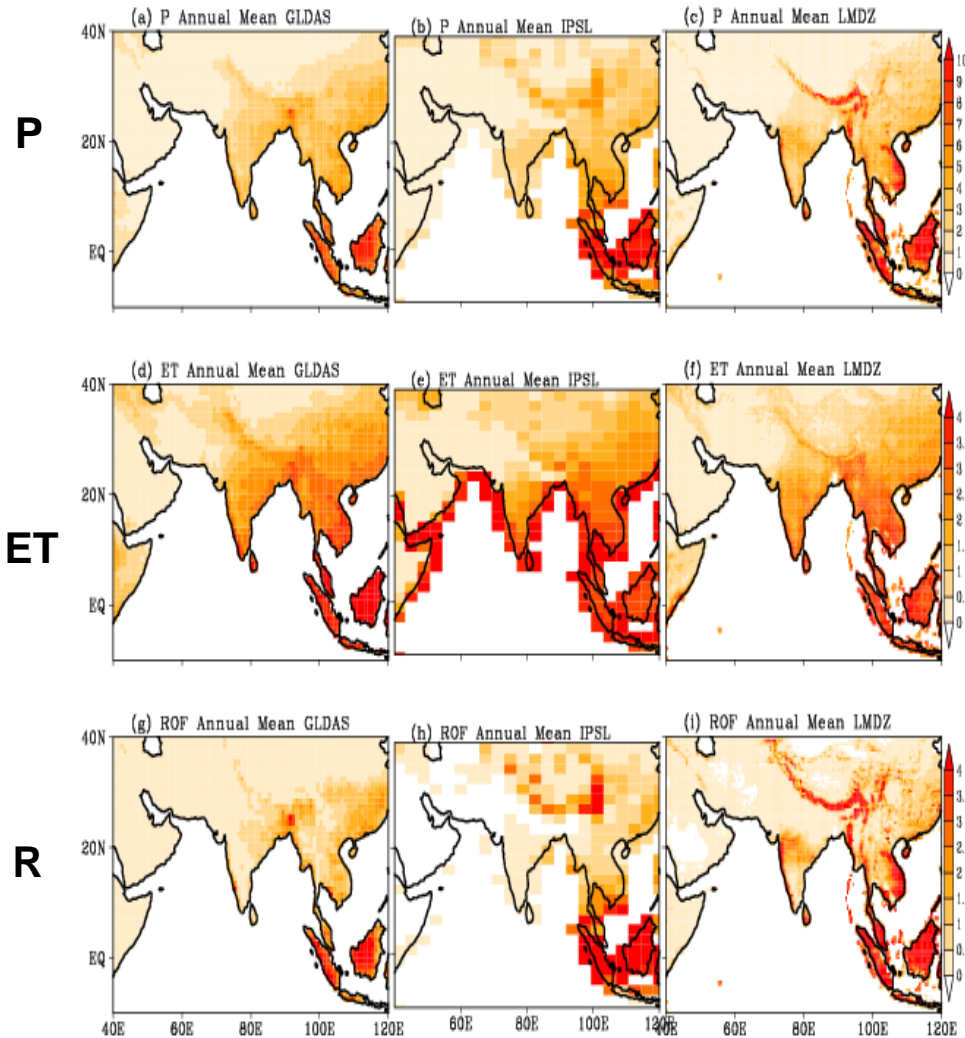
ET



Annual mean water balance (mm d⁻¹) components: (1979-2005)

GLDAS IPSL LMDZ

Water balance averaged over
70°-90°E; 10°-28°N



	GLDAS	IPSL	LMDZ
P	2.63	1.81	2.97
ET	1.99	2.25	1.92
R	0.65	0.28	1.06
P-ET	0.64	-0.44	1.05

The water balance is highlighted

Source: MVS. Ramarao, R. Krishnan
J. Sanjay, TP. Sabin (2015): ESD

High-resolution (~ 35 km) modeling of climate change over S.Asia

Historical (1886-2005):

Includes natural and anthropogenic (GHG, aerosols, land cover etc) climate forcing during the historical period (1886 – 2005) ~ 120 years

Historical Natural (1886 – 2005):

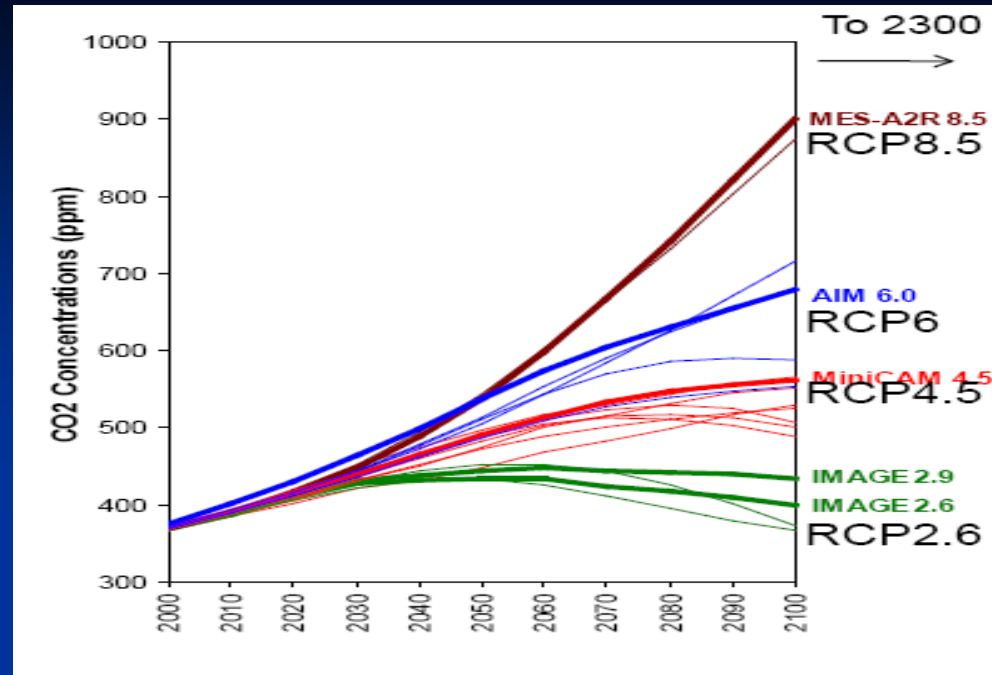
Includes only natural climate forcing during the historical period (1886– 2005) ~ 120 yrs

RCP 4.5 scenario (2006-2100) ~ 95 years:

Future projection run which includes both natural and anthropogenic forcing based on the IPCC AR5 RCP4.5 climate scenario. The evolution of GHG and anthropogenic aerosols in RCP4.5 produces a global radiative forcing of + 4.5 W m⁻² by 2100

Runs performed on PRITHVI, CCCR-IITM

CO2 concentration in future IPCC AR5 scenarios



Aerosol distribution from IPSL ESM

INCA: Interaction with Chemistry and Aerosol

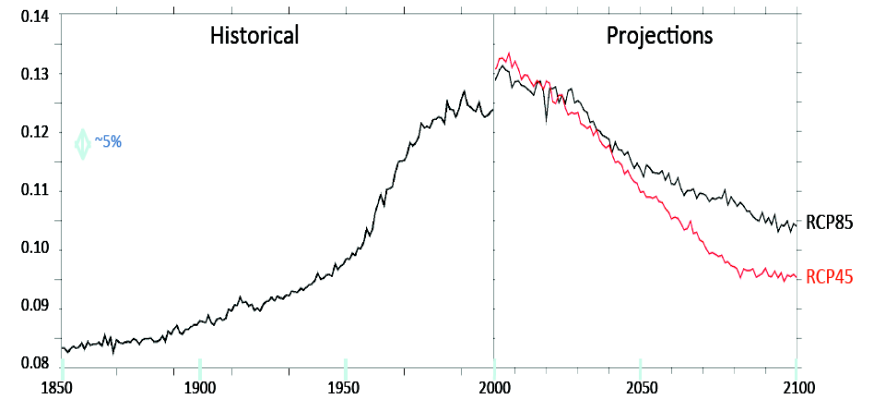
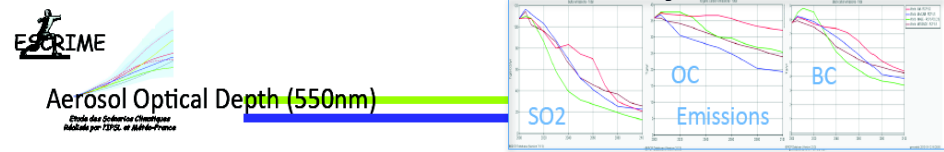
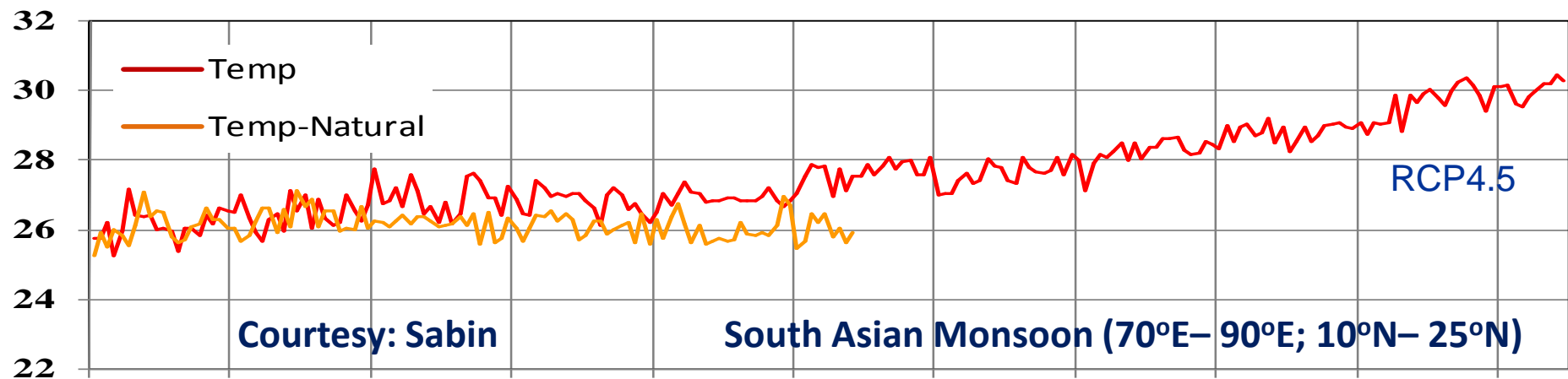
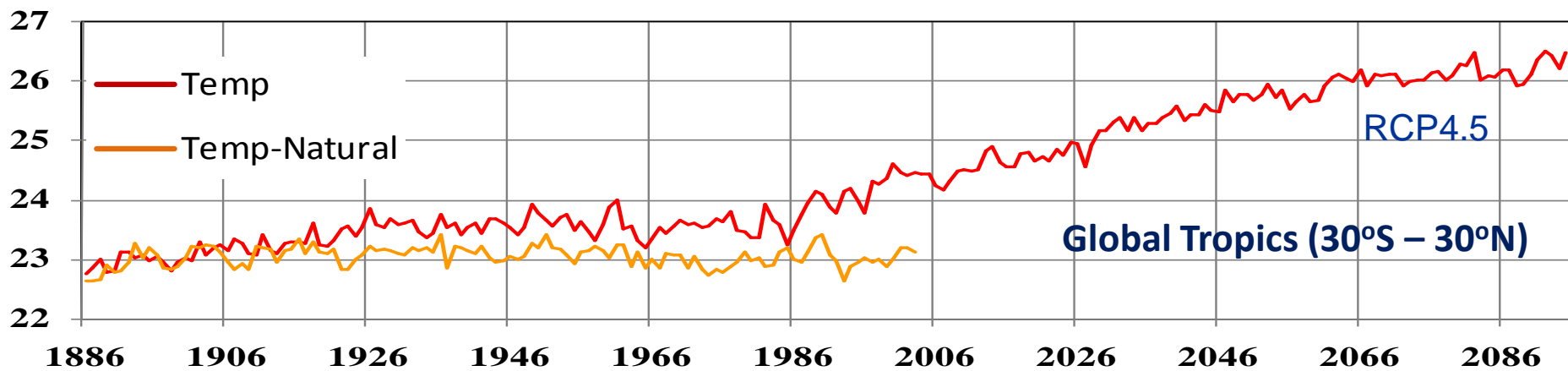
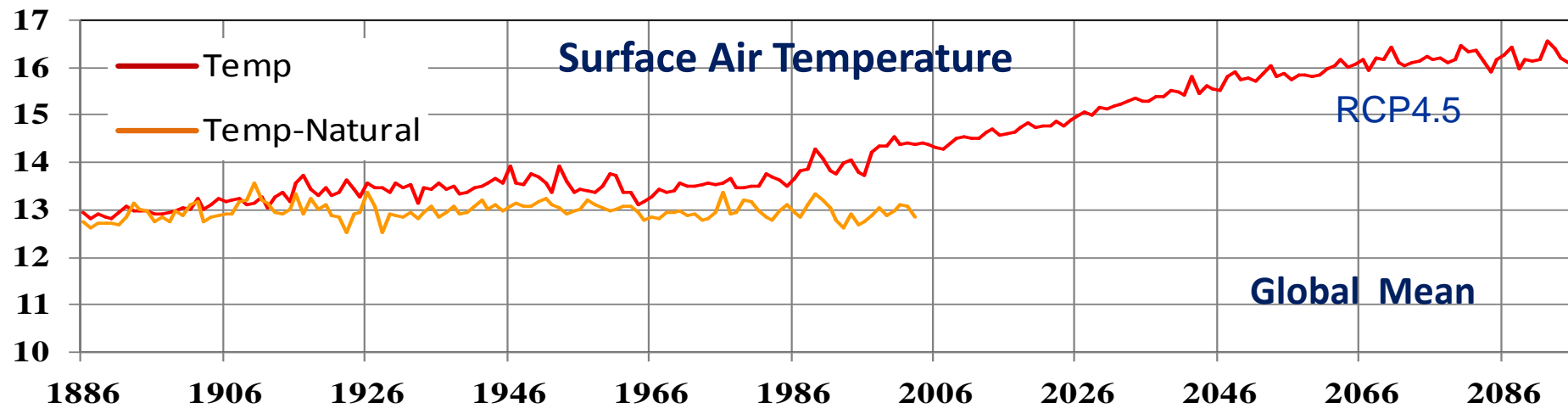
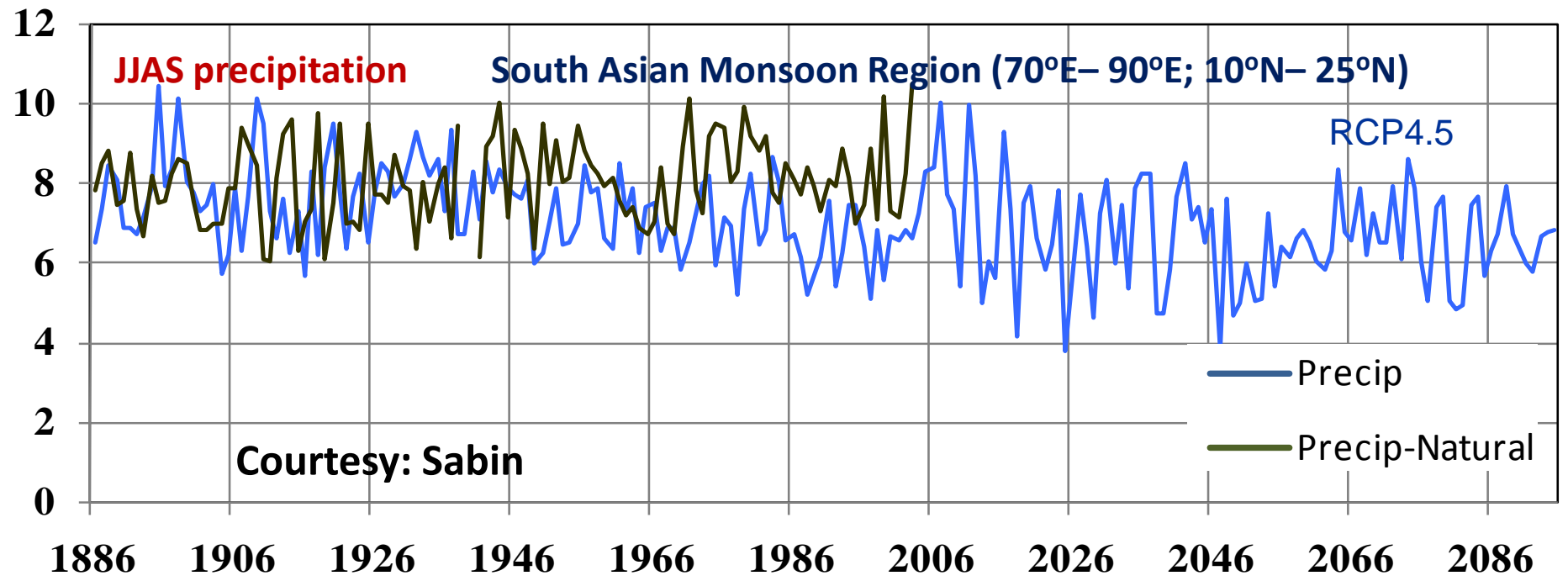
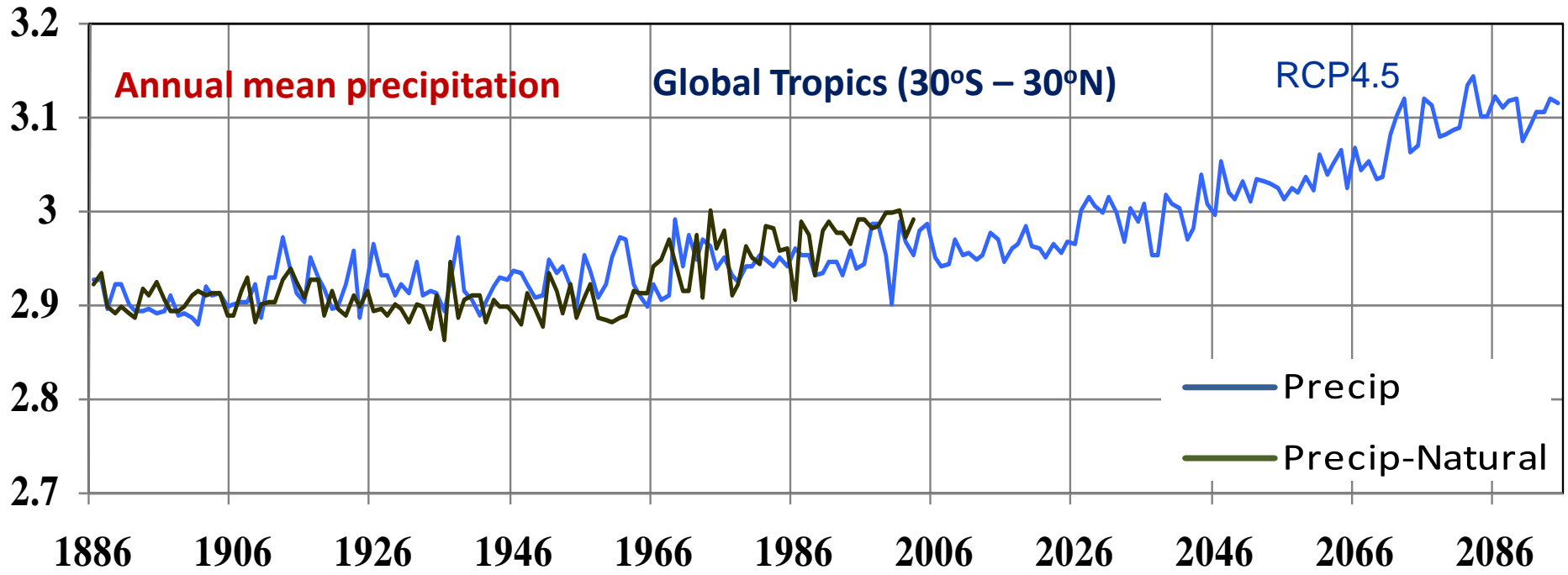
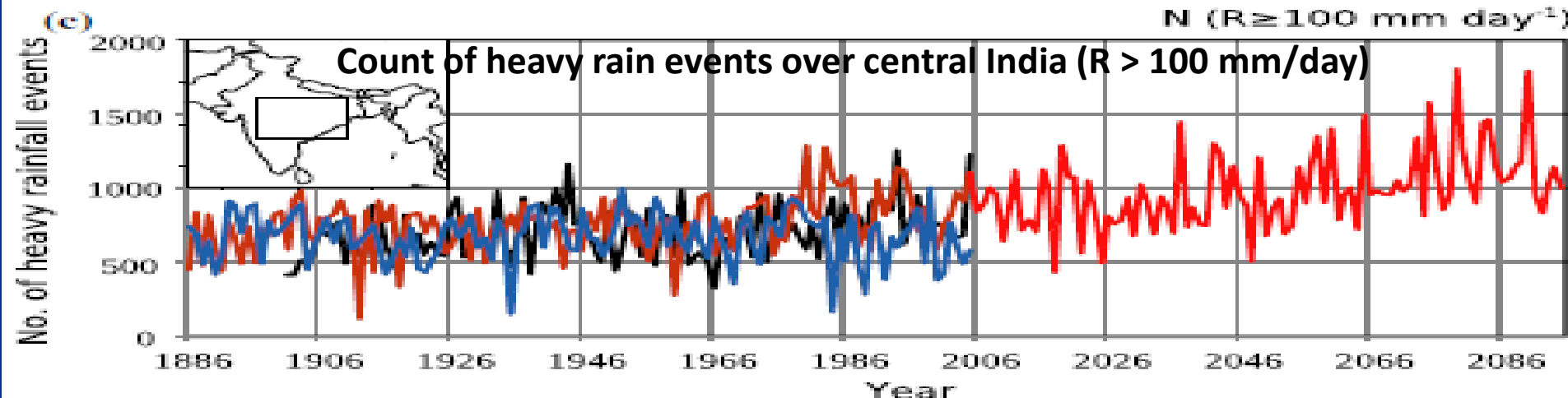
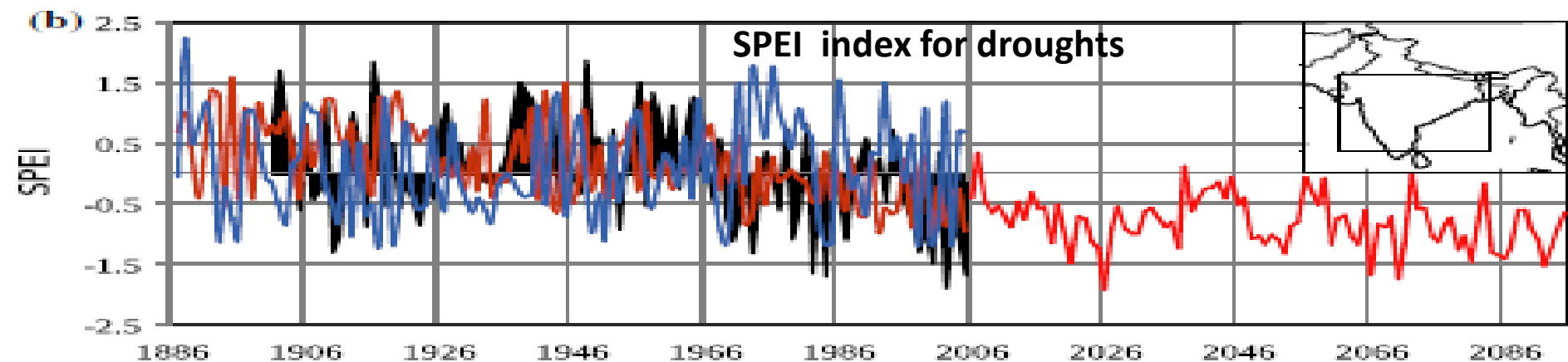
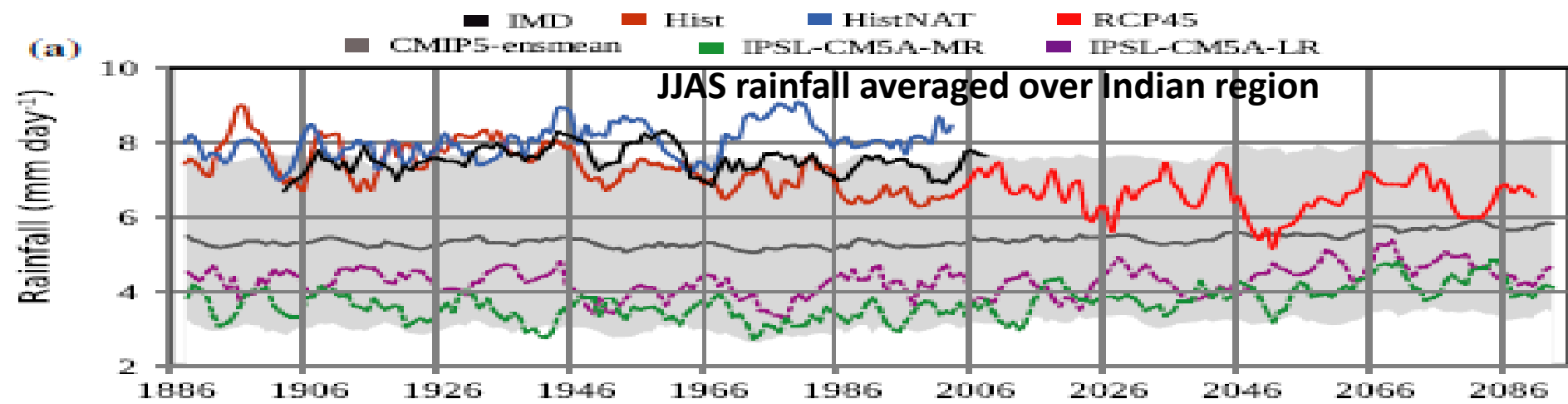


Table 2 Summary of the LMDZ4 experimental design

Expt.	Period	Forcing	Cumulus convection	SST forcing
HIST1	Historical: (1886 – 2005)	Natural and Anthropogenic forcings	Emanuel	SST_ANOM_IPSL_CM5A_HIST + SST_AMP_CLIM
HISTNAT1	Historical: (1886 - 2005)	Natural only	Emanuel	SST_ANOM_IPSL_CM5A_HISTNAT + SST_AMP_CLIM
HIST2	Historical: (1950 – 2005)	Natural and Anthropogenic forcings	Tiedtke	SST_ANOM_IPSL_CM5A_HIST + SST_AMP_CLIM
HISTNAT2	Historical: (1950 – 2005)	Natural only	Tiedtke	SST_ANOM_IPSL_CM5A_HISTNAT + SST_AMP_CLIM
RCP4.5	Future RCP4.5 scenario (2006 – 2095)	Natural and Anthropogenic forcings	Emanuel	SST_ANOM_IPSL_CM5A_RCP4.5 + SST_AMP_CLIM
HIST1_GHG	Historical (1950 – 2000) Decadal time slice runs for (1951-1960), (1961-1970), (1971-1980), (1981-1990), (1991-2000)	Natural and GHG-only forcings. Land use and aerosol fields are set to 1886 values	Emanuel	SST_ANOM_IPSL_CM5A_HIST_GHG + SST_AMP_CLIM
HIST1_PIGHG	Historical: Decadal time slice runs for (1951-1960), (1961-1970), (1971-1980), (1981-1990), (1991-2000)	Includes Natural variations, Aerosol forcing and Land-use change. The concentration of GHGs are set to 1886	Emanuel	SST_ANOM_IPSL_CM5A_HIST + SST_AMP_CLIM







Spatial map of JJAS rainfall trends (1951-2005). Units $\text{mm day}^{-1} (55 \text{ yr})^{-1}$

Time-series (1951-2005): JJAS rainfall averaged (70-90E; 10-28N)

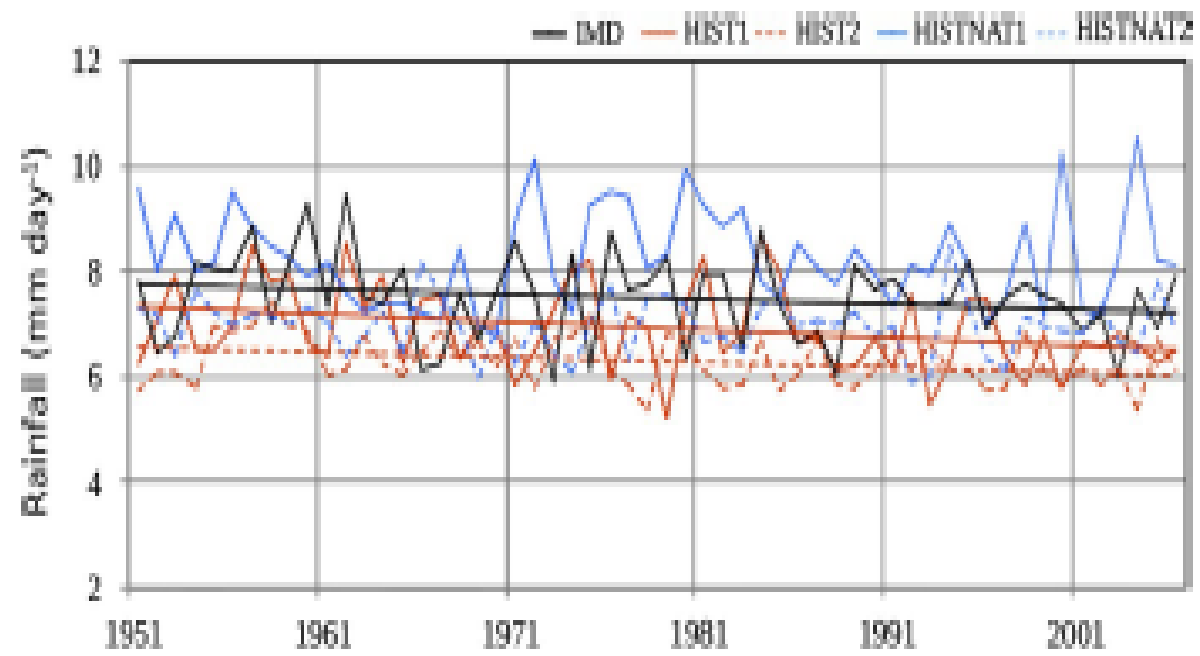
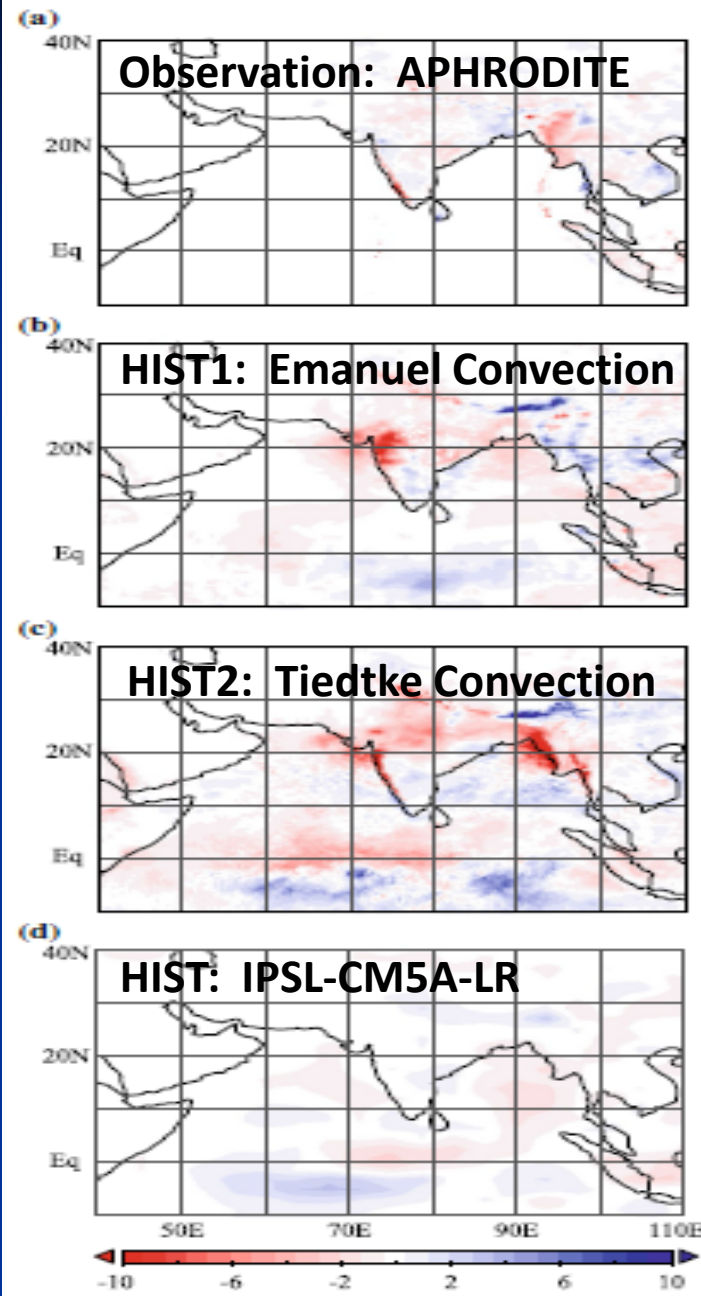
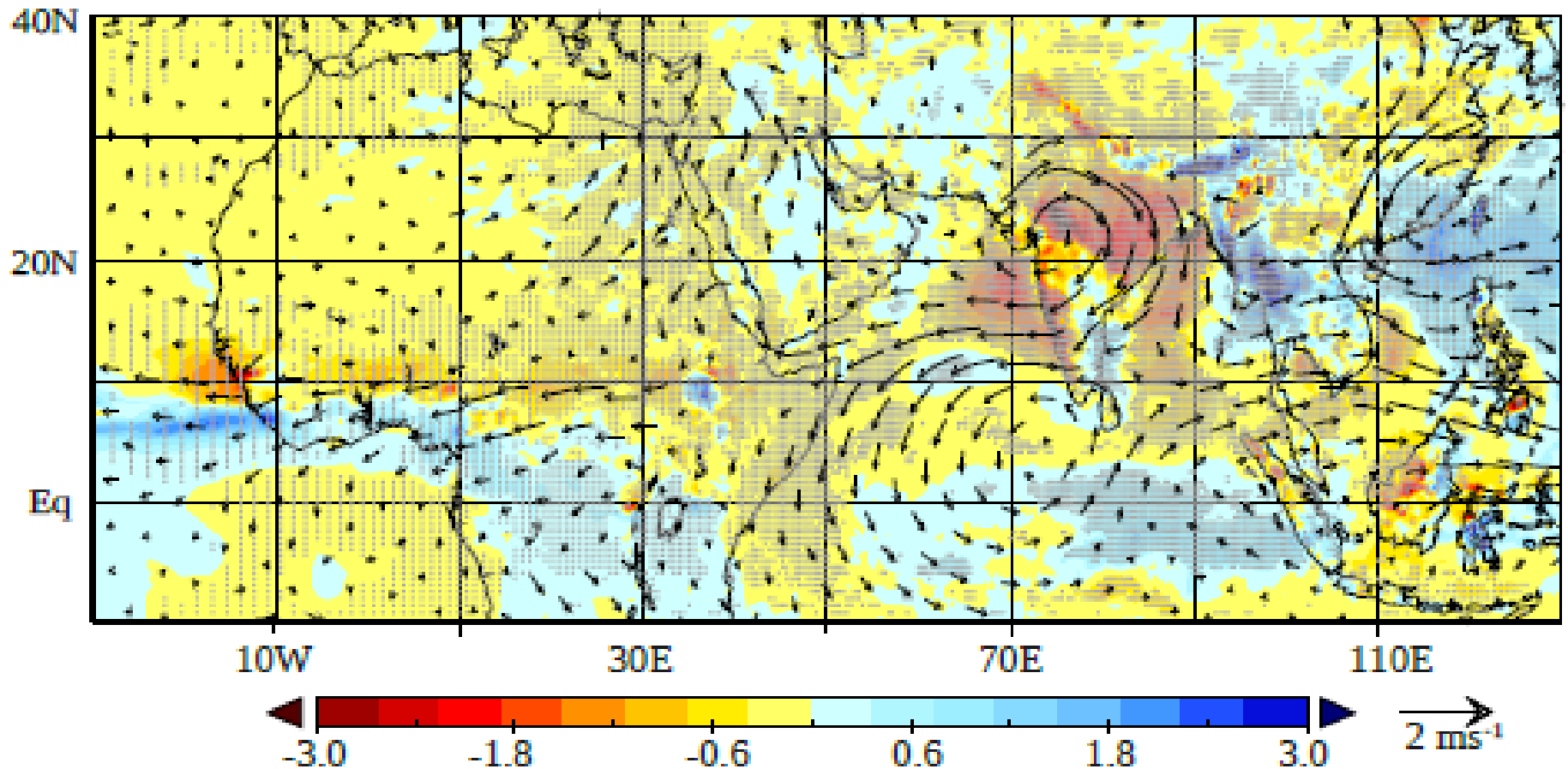


Table 1 Summary of trends of JJAS rainfall averaged over the land points for the Indian region (70° - 90° E, 10° - 28° N)

	Rainfall trend	Mean rainfall (mm day^{-1})	% change w.r.t mean rainfall	<i>P</i> value based on two tailed student's <i>t</i> test
IMD dataset (1951-2005)	$-0.55 \text{ units mm day}^{-1} (55 \text{ years})^{-1}$	7.5	-7	<0.01
HIST1 (1951-2005)	$-1.1 \text{ units mm day}^{-1} (55 \text{ years})^{-1}$	6.9	-16	<0.01
HIST2 (1951-2005)	$-0.55 \text{ units mm day}^{-1} (55 \text{ years})^{-1}$	6.3	-9	<0.01
HISTNAT1 (1951-2005)	$-0.03 \text{ units mm day}^{-1} (55 \text{ years})^{-1}$	8.3	-0.3	0.54 (not significant)
HISTNAT2 (1951-2005)	$-0.1 \text{ units mm day}^{-1} (55 \text{ years})^{-1}$	6.9	-1	0.2 (not significant)
RCP4.5 (2006-2060)	$-1.1 \text{ units mm day}^{-1} (55 \text{ years})^{-1}$	6.6	-17	<0.01
RCP4.5 (2006-2095)	$-0.29 \text{ units mm day}^{-1} (90 \text{ years})^{-1}$	6.6	-5	<0.01

Mean difference maps (All-forcing minus Natural) during 1951-2005

JJAS rainfall and 850 hPa winds



Decomposing the monsoon response to GHG and regional forcing

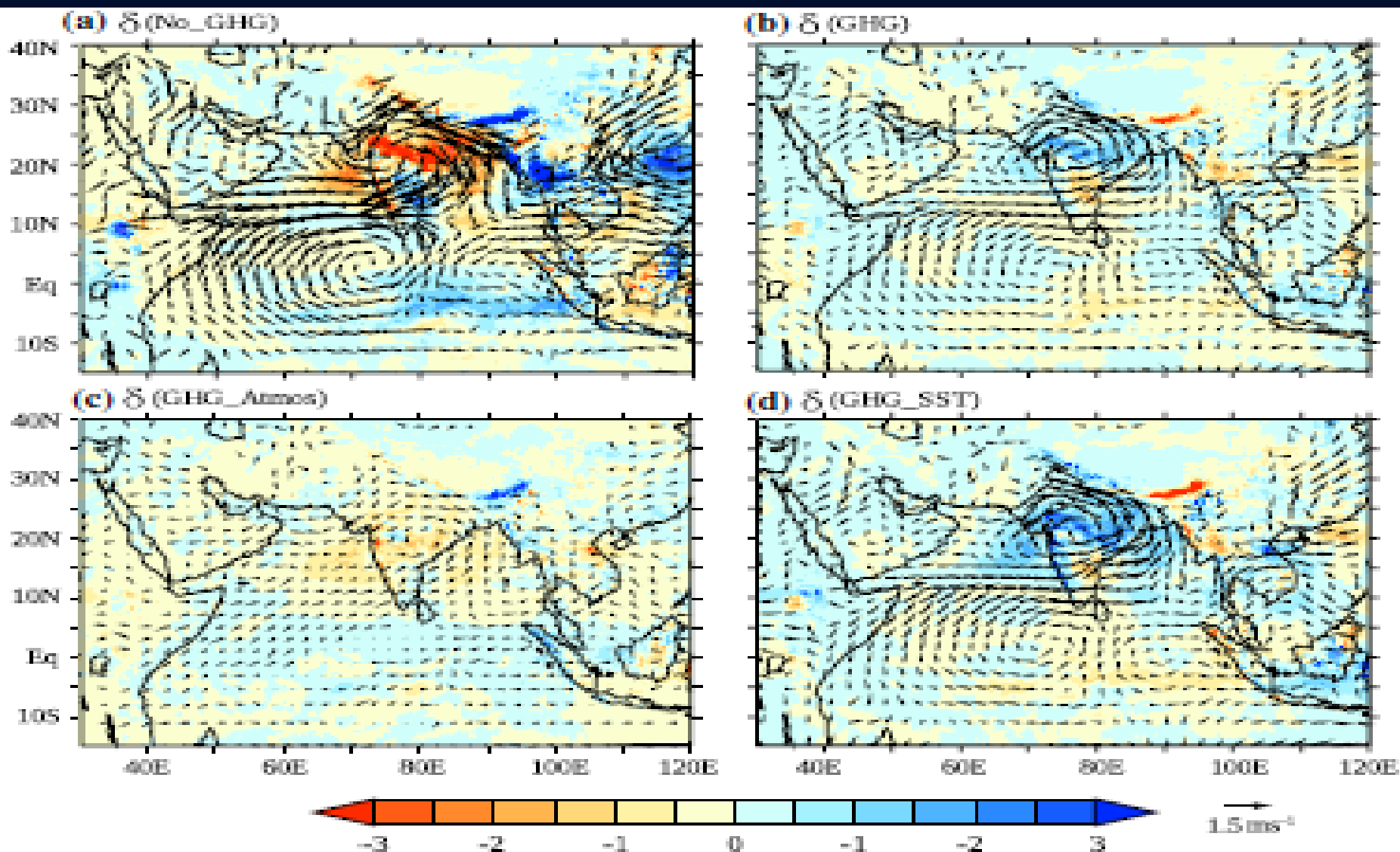


Fig. 6 Decomposing the monsoonal response to GHG and regional forcing elements Composite difference maps of the simulated June-September precipitation (mm day^{-1}) and 850 hPa winds (ms^{-1}), a $\delta(\text{No_GHG}) = \text{HIST1} - \text{HIST1_GHG}$, b $\delta(\text{GHG}) = \text{HIST1_}$

$\text{GHG} - \text{HISTNAT1}$, c $\delta(\text{GHG_Atmos}) = \text{HIST1} - \text{HIST1_PIGHG}$, d $\delta(\text{GHG_SST}) = \delta(\text{GHG}) - \delta(\text{GHG_Atmos})$. The composite maps are constructed for the period (1951-2000) using the decadal time-slices

(HIST minus HISTNAT): 1951-2002

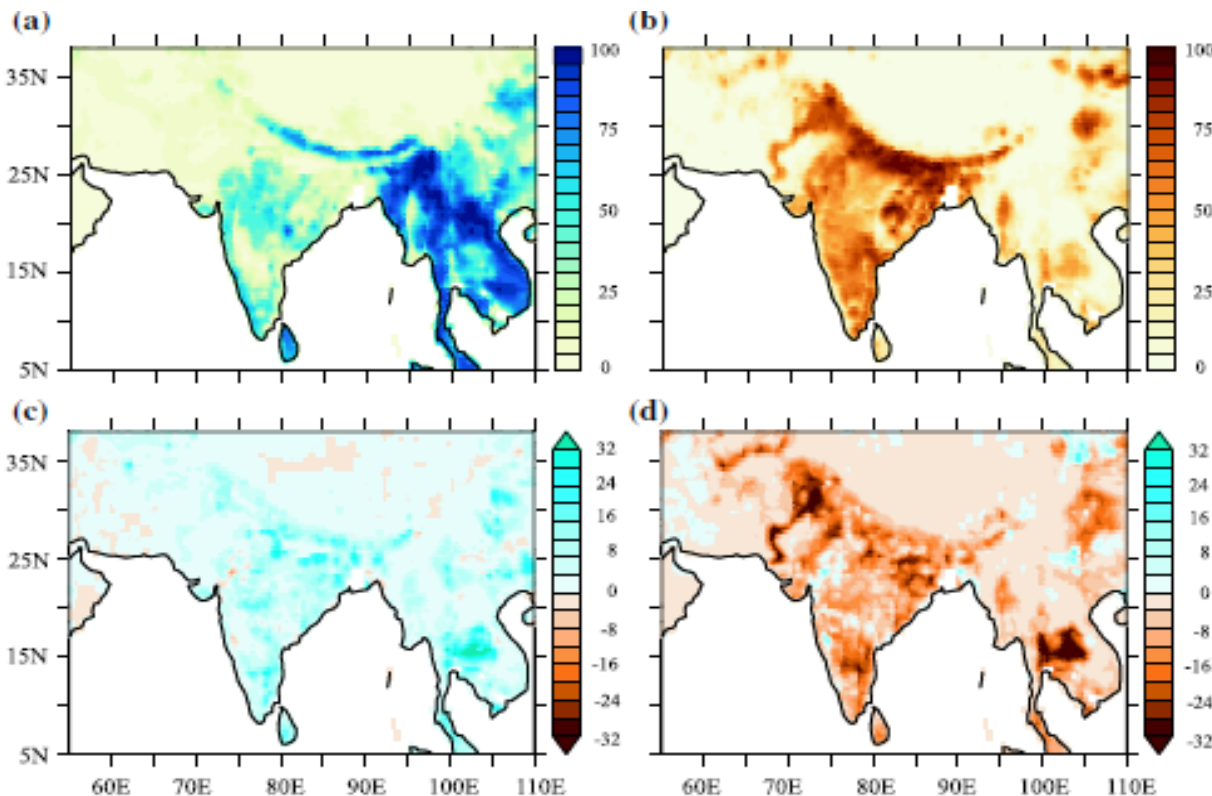
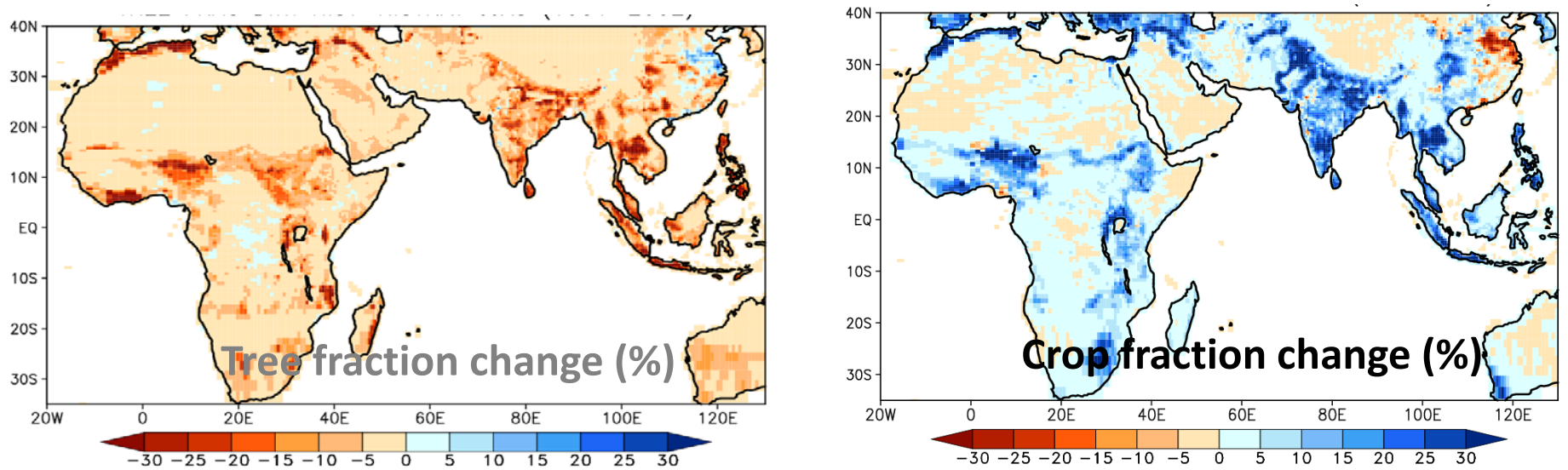


Fig. 8 Spatial maps of land-use used in the LMDZ4 experiments. **a** Mean tree-fraction (%) for the period 1951–2000. **b** Same as **a** except for crop-fraction (%). **c** Change in tree-fraction (%) shown by difference [(1891–1930) minus (1951–2000)] map. **d** Same as **c** except for crop-fraction (%). Note the larger spatial coverage of tree area over South and Southeast Asia and China during (1891–1930) relative to (1951–2000); while the crop area coverage was less during (1891–1930) relative to (1951–2000)

Map of JJAS SST trend (1951-2005)

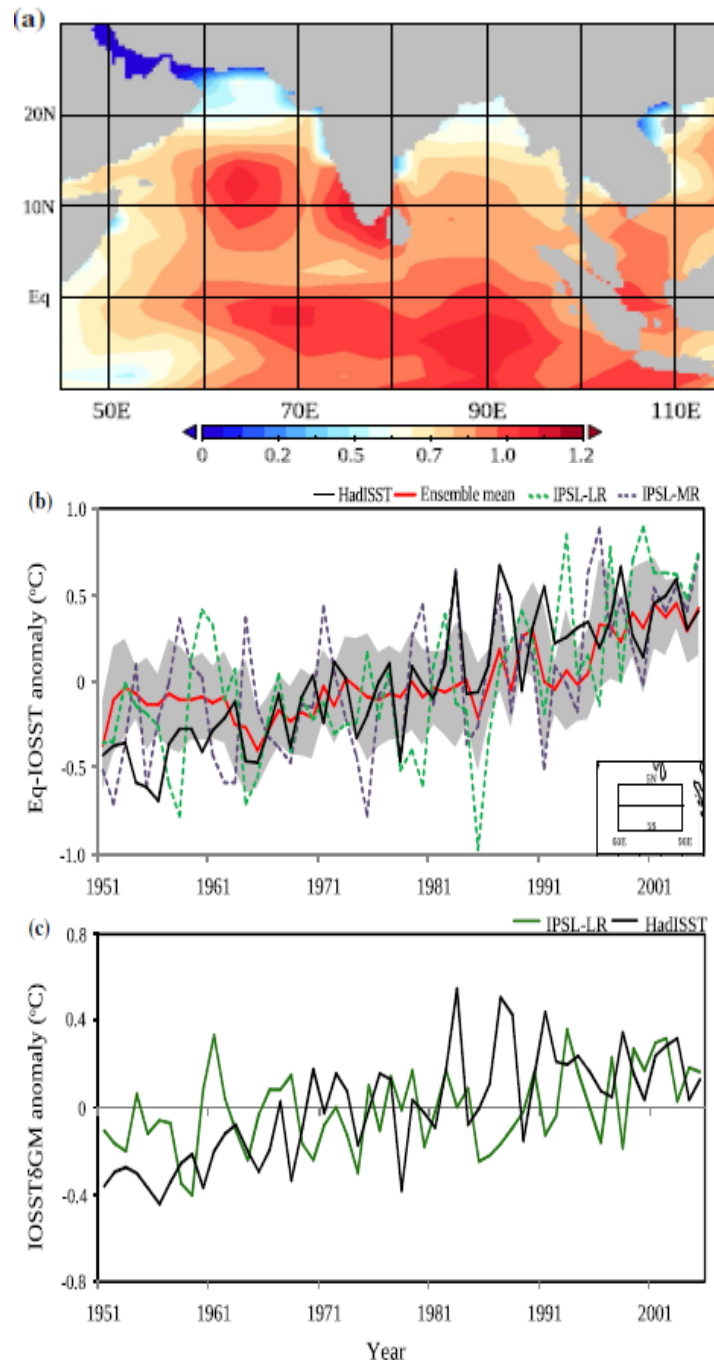
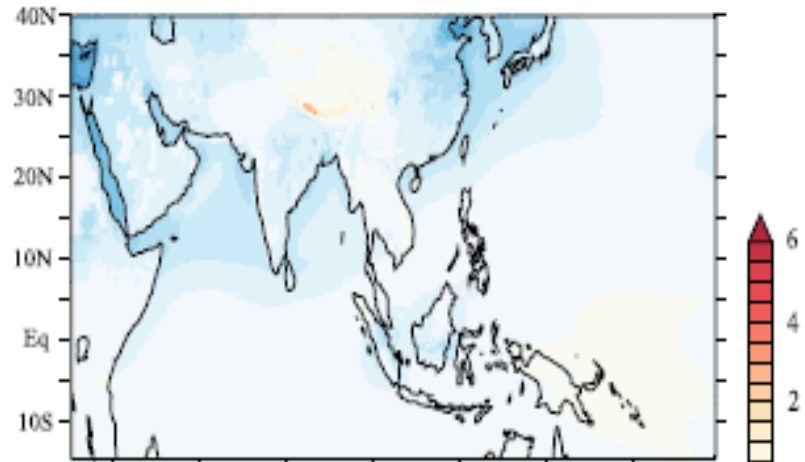


Fig. 10 Tropical Indian Ocean SST warming trend during (1951-2005). **a** Spatial pattern of linear trend of SST ($^{\circ}\text{C}$ per 55 years) from the IPSL-CM5A-LR simulation. **b** Time-series of equatorial Indian Ocean SST (IOSST in $^{\circ}\text{C}$) anomalies averaged over the region (5°S - 5°N , 60° - 90°E) from HadISST (black line), IPSL-CM5A-LR (green line), IPSL-CM5A-MR (purple), ensemble mean of CMIP5 models (red line). The grey shading shows the spread of SST anomalies simulated across the CMIP5 models. **c** Time-series of IOSST&GM anomalies ($^{\circ}\text{C}$) (IOSST&GM = EQIOSST minus Global Mean SST) for HadISST (black line), IPSL-CM5A-LR (green line). The rapid warming of IOSST&GM is apparently linked to weakening of the summer-monsoon cross-equatorial flow in recent decades (Swapna et al. 2014)

(a) Anthropogenic Aerosol Forcing @ TOA



(b) Atmospheric absorption (TOA - SFC)

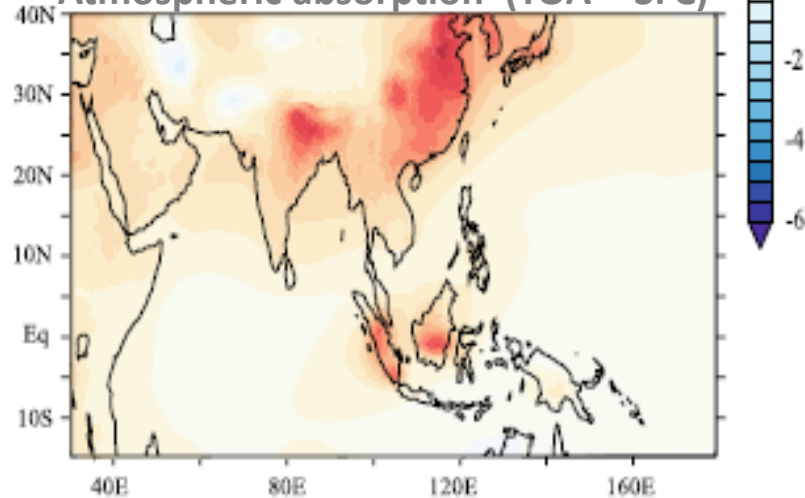


Fig. 9 Spatial distribution of mean anthropogenic aerosol forcing from the HIST1 experiment during 1951-2005. **a** Anthropogenic aerosol forcing (Wm^{-2}) at the top-of-atmosphere (TOA). **b** Atmospheric absorption (Wm^{-2}) due to anthropogenic aerosols (i.e., aerosol-forcing @ TOA minus aerosol-forcing @ Surface). The mean aerosol forcing is computed for the JJAS season from the HIST1 simulation during the period 1951-2005

Long term trends of SST and surface winds over the Tropical Indian Ocean

P. Swapna, R. Krishnan & J. M. Wallace, *Climate Dynamics*, 2013

June – September (JJAS)

Rest of the year

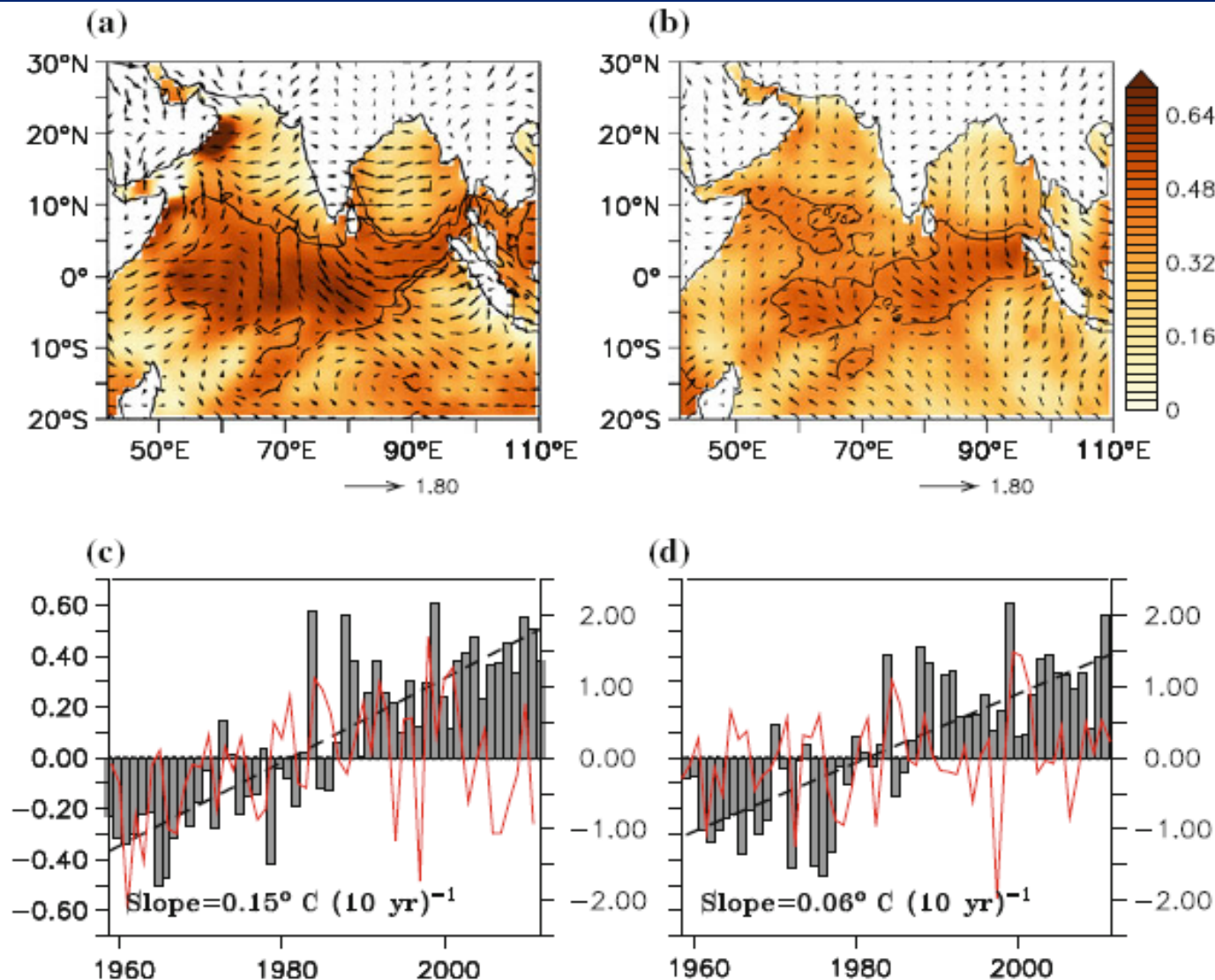
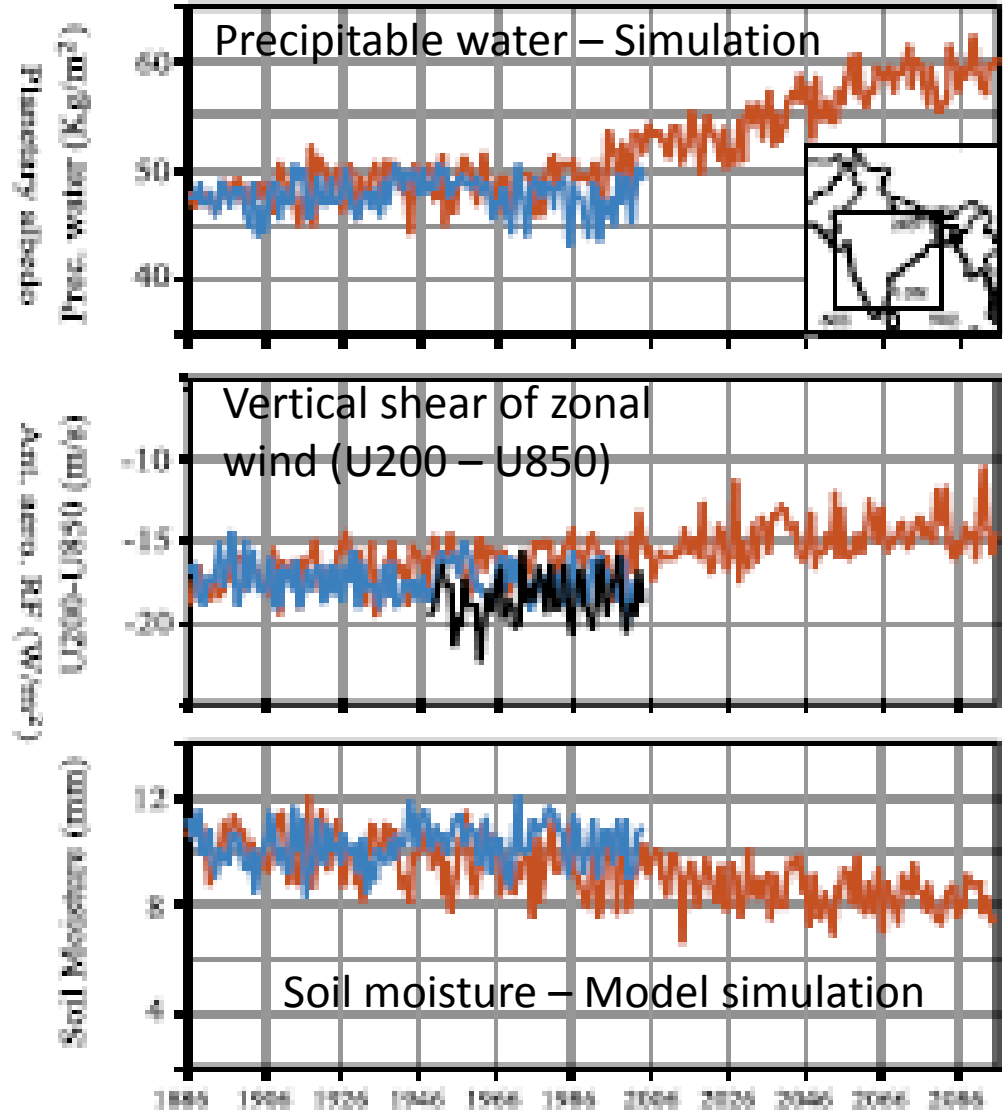
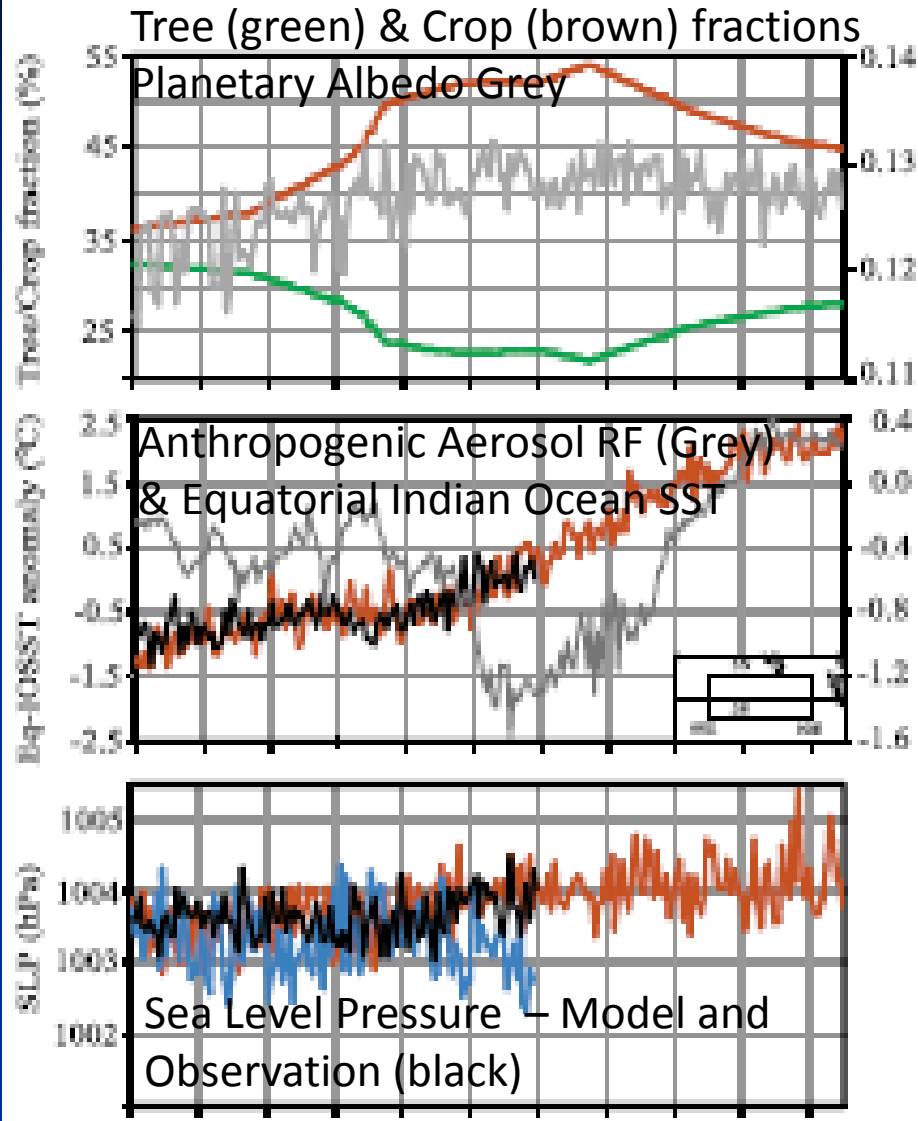


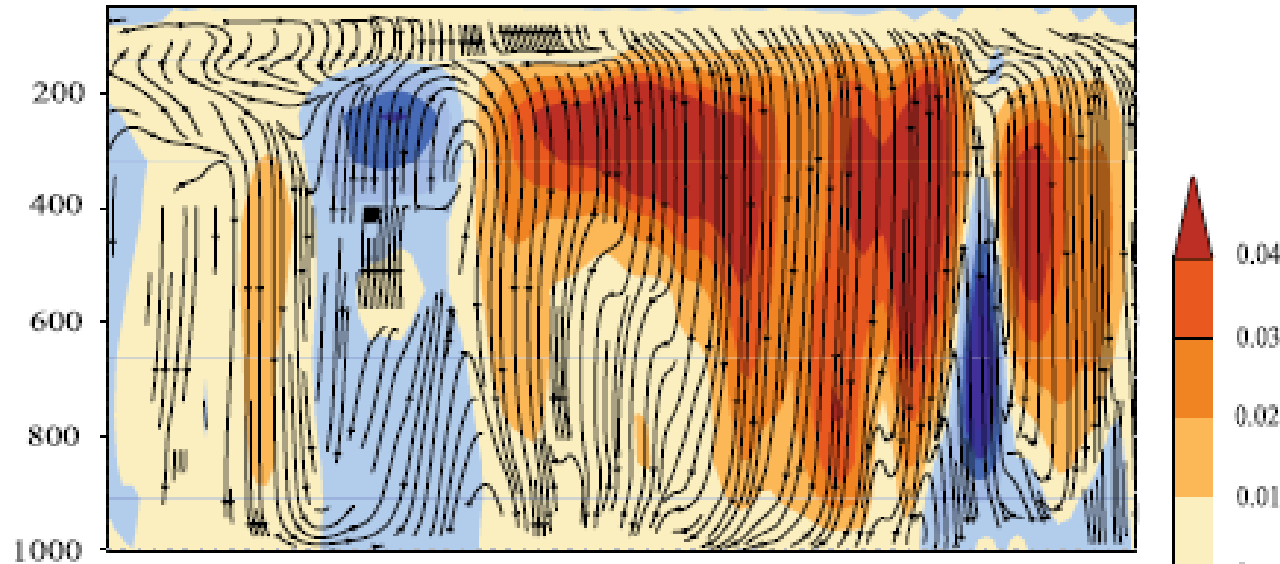
Fig. 1 Upper panels show trends in sea surface temperature (SST in °C per 62 years; the departure from the global mean SST) and ERA surface winds (m s⁻¹ per 54 years) in the tropical Indian Ocean (IO) for the summer monsoon season. **a** June–September; **b** the remaining calendar months. Color shading indicates the magnitude of SST trends and the contour corresponds to 99 % confidence level based on the Student's *t* test (see Balling et al. 1998). The lower panels show time-series of SST (°C) bars and ERA zonal wind anomalies (m s⁻¹, red lines) averaged over the equatorial IO (50°E–100°E, 5°S–5°N). **c** June–September and **d** the remaining calendar months. The trends of the linear regression best-fit lines exceed the 95 % confidence level

Time-series of regional forcing & simulated response

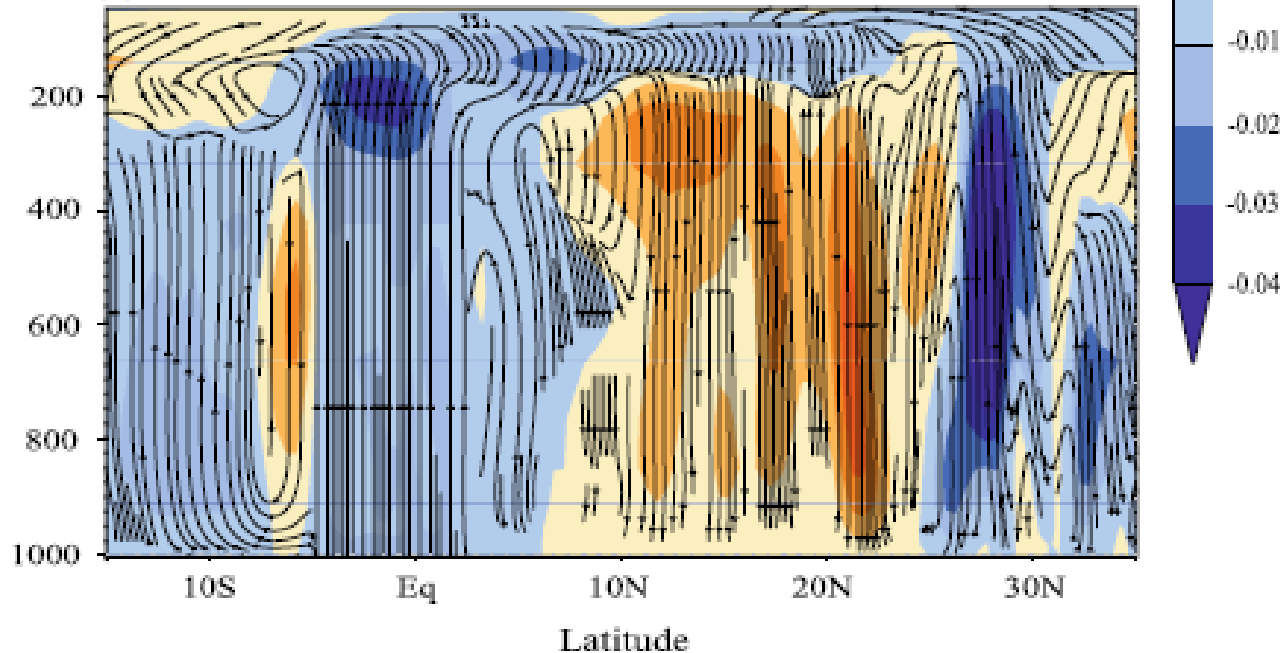


Weakening of monsoon Hadley-type overturning

(a) Hist1-HistNAT1



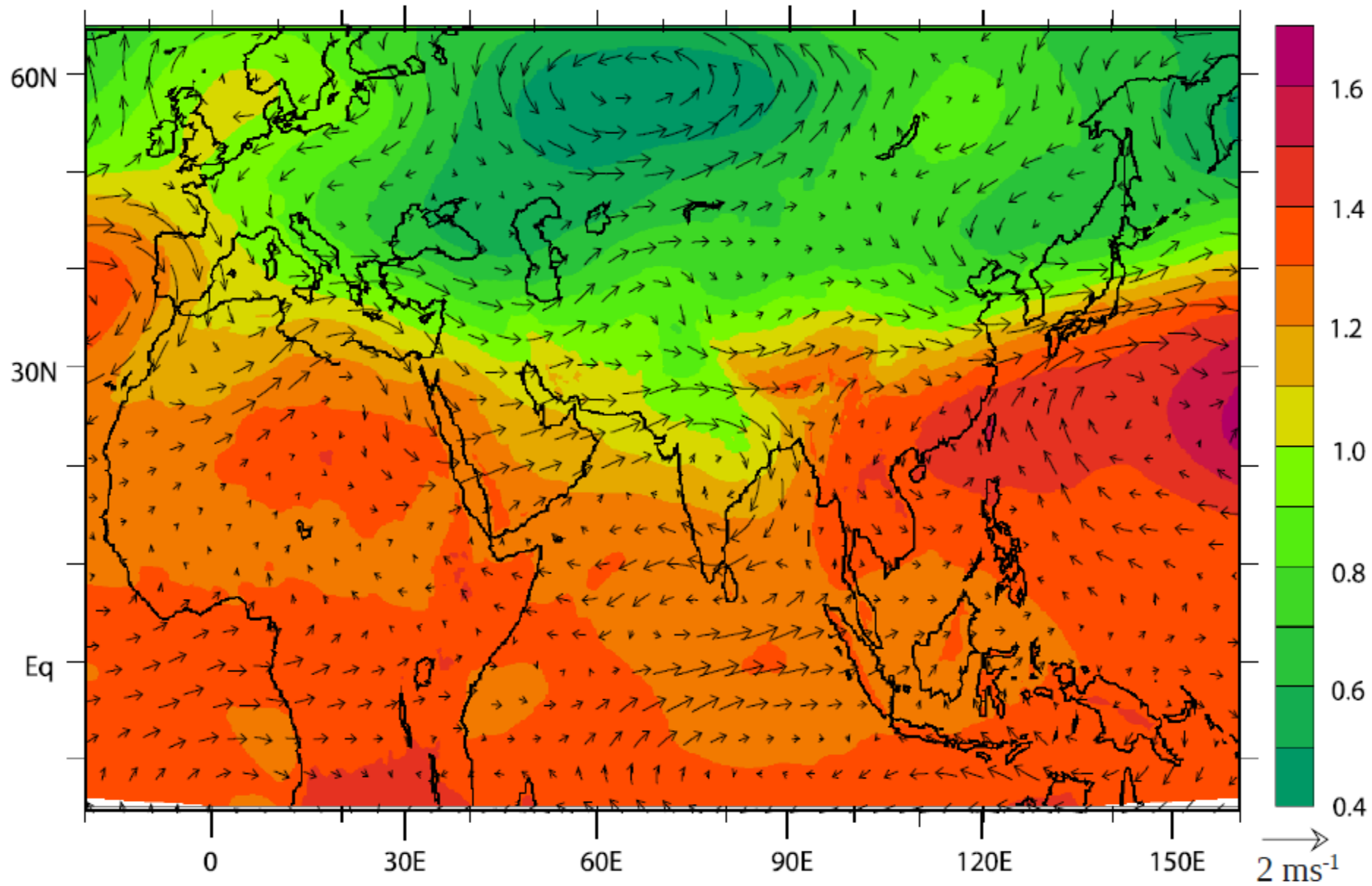
(b) RCP4.5-Hist1



Latitude Pressure
sections of difference
plots of meridional
overturning
circulation anomalies

Response of tropospheric temperature & large-scale circulation to Anthropogenic forcing

IST minus HISTNAT (1951 - 2005): Winds & temperature vertically averaged 600-200 hPa



Time-series of year-wise count of heavy rain events (intensity > 100 mm/day) over Central India

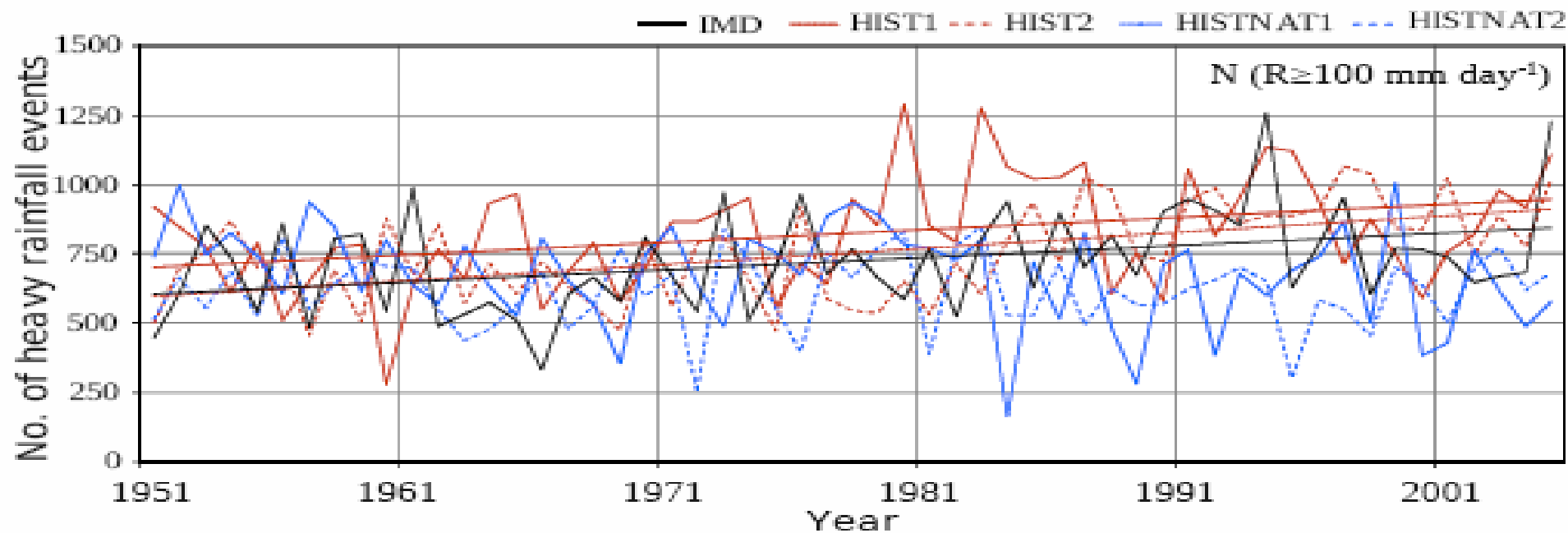
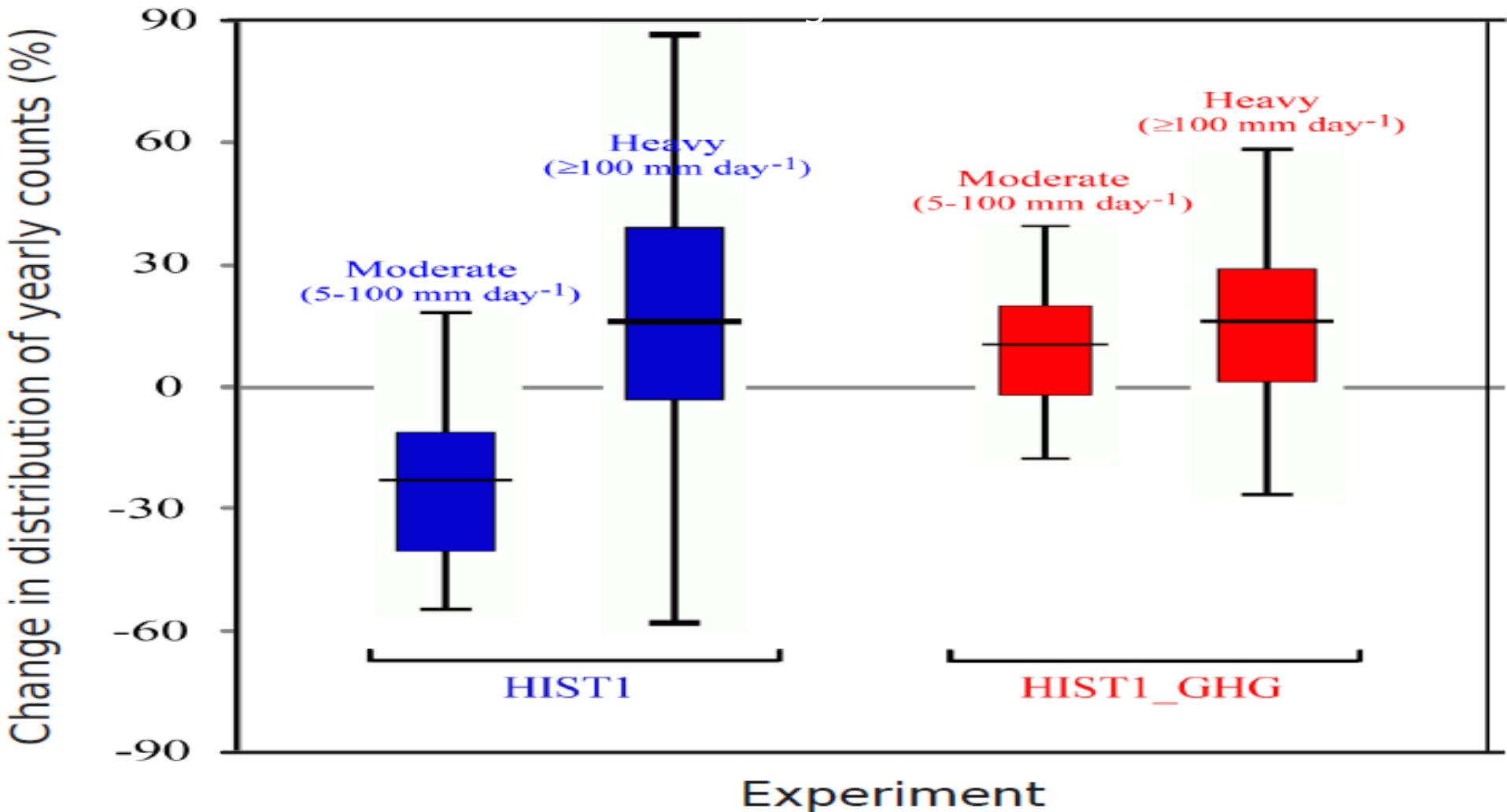


Table 4 Summary of trends in the frequency of heavy precipitation events over Central India, with intensities $\geq 100 \text{ mm day}^{-1}$, from IMD observations and LMDZ4 simulations

	Trend in the frequency count	Mean frequency count	% change w.r.t mean frequency count	<i>P</i> value based on the two tailed student's <i>t</i> test
IMD dataset (1951–2005)	430 units (55 years) ⁻¹	1448	30	<0.01
HIST1 (1951–2005)	499 units (55 years) ⁻¹	1652	30	<0.01
HIST2 (1951–2005)	638 units (55 years) ⁻¹	1507	42	<0.01
HISTNAT1 (1951–2005)	-34 units (55 years) ⁻¹	1356	-3	0.2 (not significant)
HISTNAT2 (1951–2005)	+6 units (55 years) ⁻¹	1233	0.5	0.8 (not significant)
RCP4.5 (2006–2095)	750 units (90 years) ⁻¹	1976	38	<0.01

Changes in Heavy & Moderate precipitation types to GHG & regional



Central India: 74.5°E – 86.5°E, 16.5°N - 26.5°N

Period:1951-2000

Frequency counts for both categories are relative to HISNAT

Summary

- Response of South Asian monsoon to climate change is examined using a zoomed version of LMDZ, forced by SST, without lateral boundary condition
- High resolution improves mean monsoon simulation - precipitation and interactions between precipitation and atmospheric circulation
- Long-term climate change experiments using the high-resolution LMDZ model highlight several value additions as compared to coarse resolution simulations
- The simulation with anthropogenic forcing captures the decreasing trend of S. Asian monsoon precipitation in the post-1950s . A 21st century projection based on the RCP4.5 scenario indicates further decline of monsoon rainfall, persistent drought conditions and soil moisture decrease in the coming decades.
- Results indicate the role of regional forcing elements (ie., land cover change, anthropogenic aerosols, equatorial IO SST warming) on the recent monsoon decline.
- An increase of regional planetary albedo by about 9% is seen in the simulation during 1886-2005, which allows of suppression of monsoon precipitation through enhanced subsidence over the S. Asian region
- Robust increase in frequency of heavy precipitation ($R > 100$ mm/day) occurrences over Central India is noted in the high-resolution simulation

Coupled variability of monsoon precipitation and low level winds (1951-2005)

